Path Tracking with a Bounded–Curvature Vehicle: a Hybrid Control Approach.

Andrea Balluchi[†], Antonio Bicchi[§], Philippe Souères[‡]

†PARADES, Via di S.Pantaleo, 66, 00186 Roma, Italy. balluchi@parades.rm.cnr.it, fax: +39 06 68807926

§Centro Interdipartimentale di Ricerca "Enrico Piaggio". Università di Pisa, 56100 Pisa, Italy, bicchi@ing.unipi.it

‡Laboratoire d'Analyse et d'Architecture des Systèmes – LAAS,

CNRS, 7, Avenue du Colonel Roche, 31077 Toulouse, France. soueres@laas.fr

Abstract

In this paper, we consider the problem of stabilizing the kinematic model of a car to a path in the plane under rather general conditions. The path is subject to very mild restrictions, while the car model, although rather simplified, contains the most relevant limitations inherent in wheeled robots kinematics. Namely, the car can only move forward, its steering radius is lower bounder and a limited sensory information only provides a partial knowledge of some state parameters. In particular, we consider the case that the current distance and the heading angle error with respect to the closest point on the reference path can be measured but only the sign of the path curvature is detected.

These constraints are such to make classical control techniques inefficient. The proposed approach is based on an extensions of optimal synthesis results successfully applied in a previous work for tracking rectilinear paths. Due to both the nature of the problem, and the solution technique used, the analysis of the controlled system involves a rather complex switching logic. Hybrid formalism and verification techniques prove extremely useful in this context to formally proof stability of the resulting system, and are described in detail in the paper. The practicality of the proposed approach, in spite of nonidealities in real-world applications, is finally demonstrated by reporting experimental results.

Keywords: nonholonomic vehicles, path tracking, hybrid systems.

1 Introduction

In this paper we consider the design of a control law for path tracking by a so–called Dubins' model of a car. Dubins' car is the kinematic model of a wheeled (nonholonomic) vehicle that moves only forwards in a plane, and possesses a lower–bounded turning radius. The model is relevant to the kinematics of road vehicles as well as aircraft cruising at constant altitude, or sea vessels.

Although the design of control techniques for nonholonomic vehicles has been the subject of extensive research recently (see e.g. [12, 14, 7]), the additional constraint that the steering radius of the vehicle is lower bounded has not been explicitly considered. However, such a restriction appears to be crucial in making a kinematic model of a car relevant to real–world vehicles encountered in most applications. Another important assumption often used in the literature is that the full state of the system is available for measurement, and that the path to be tracked is entirely known in advance. Instead, we consider in this paper the more realistic and less demanding case that the vehicle can only measure its current distance and heading angle error with respect to the closest point on the reference path in the plane, where only the sign of the path curvature is detected.

The approach we follow to stabilization of Dubins' cars is to adapt to the present general case an optimal synthesis approach successfully applied in our previous work to tracking rectilinear paths [13]. Due to both the nature of the problem, the type of sensors, and the solution technique used, the analysis of the controlled system involves a rather complex switching logic. Hybrid formalism (see [6, 16, 2]) and verification techniques (see [9, 8, 1]) are extremely useful in this context to formally proof stability of the resulting system.

This paper is organized as follows. In Section 2, a hybrid automaton that describes the motion of the vehicle with respect to the path is introduced, while in Section 3 the path–tracking controller is developed. Such

controller, described in detail in Section 3.2, is obtained by considering a local approximation of the desired path with the tangent line, and by using a feedback controller designed for stabilization on straight paths (reported in Section 3.1). The advantages of the novel hybrid path–tracking formalization are exploited in Section 4, where the stability properties of the proposed controller are investigated. By a reachability analysis in the continuous state space, a finite state abstract representation of the hybrid closed–loop automaton is obtained. Though this representation is not a bisimulation, but rather a simulation, of the hybrid automaton ([6]), it suffices to prove the stability properties of the proposed control. It is shown that the proposed hybrid feedback controller achieves stabilization of Dubins' car on a generic reference path and sufficient conditions for global attractivity are derived. Finally, experimental results obtained by the proposed control law on a laboratory vehicle are presented in section 5, along with a discussion of practical issues in application of our algorithms.

2 Hybrid path tracking modelling using switching Frenet's frames

We consider the kinematic model of a car moving forwards on a plane, which was introduced by Dubins in [5]. A configuration of the vehicle is defined by an ordered pair $(M(x,y),\theta) \in \mathbb{R}^2 \times S^1$, where (x,y) are the coordinates of a reference point M in the plane and θ is the angle made by the direction of the car with respect to the x-axis. The kinematics of the car are described by

$$\begin{cases} \dot{x} = V\cos\theta \\ \dot{y} = V\sin\theta \\ \dot{\theta} = \omega \end{cases} \qquad \text{with} \qquad |\omega| < \frac{V}{R}, \tag{1}$$

where V is the constant forward velocity, ω the is turning speed and the input constraint models a lower bound $R > 0$ on the turning radius of the Dubins' car. The problem we are concerned with is that of steering the vehicle to a given *feasible* path Γ, defined by an arclength parameterization as

$$\Gamma = \left\{ (\hat{x},\hat{y}) \in \mathbb{R}^2 \mid (\hat{x},\hat{y}) = \hat{g}(\beta) \text{ for } \beta \in \mathbb{R} \right\}, \tag{2}$$

with the following conditions:

A) $\hat{g}(\cdot)$ is a class C^1 mapping from $\mathbb{R}$ to $\mathbb{R}^2$ and the orientation of Γ is that induced by increasing β;

B) Let $\kappa(\beta)$ denote the extension by continuity from the left[1] of the curvature of Γ, expressed as a function of the curvilinear abscissa β. There exists a positive real R_Γ such that the normalized curvature $\hat{\kappa}(s) \equiv R\kappa(s)$ satisfies

$$|\hat{\kappa}(\beta)| = R|\kappa(\beta)| \leq \frac{R}{R_\Gamma} \equiv C < 1. \tag{3}$$

C) Considering the open neighbourhood of the path

$$\mathcal{T}_\Gamma = \left\{ \mathbf{x} \in \mathbb{R}^2 : \exists \beta \in \mathbb{R}, \|\mathbf{x} - \hat{g}(\beta)\| < R_\Gamma \right\} \subset \mathbb{R}^2, \tag{4}$$

for all $\mathbf{x} \in \mathcal{T}_\Gamma$ there exists a unique nearest point on Γ.

In order to describe the motion of the vehicle with respect to the reference path Γ a mobile Frenet's frame associated to the curve Γ is considered. Given a vehicle position $M(x,y) \in \mathcal{T}_\Gamma$, the Frenet's frame $\mathcal{S}_T(s)|_{s=\bar{\beta}}$ is defined by the tangent, the principal normal and the binormal axes of the curve at the point $(\hat{x}(\bar{\beta}), \hat{y}(\bar{\beta}))$ of Γ which is at minimum distance[2] from $M(x,y)$ (see Figure 1). As the vehicle moves with velocity V, the Frenet's frame $\mathcal{S}_T(s)$ follows its motion so as to keep it on the principal normal axis. The arclength parameter s locates the current Frenet's frame. The tangent and the principal normal axes of $\mathcal{S}_T(s)$ remain within the plane containing the curve, while the binormal axis points either upwards, if the local curvature of Γ is counterclockwise (i.e. $\kappa(s) > 0$), or downwards, if the local curvature is clockwise (i.e. $\kappa(s) < 0$). Introduce the transformed coordinates $(s, \tilde{y}, \tilde{\theta})$, where:

[1] By definition, $\kappa(\beta) = \lim_{s \to \beta^-} \kappa(s)$, at points $(x(\beta), y(\beta))$ where the curvature of Γ is not defined.

[2] Note that, by *A*), *B*) and *C*), the Frenet's frame is well-defined along Γ.

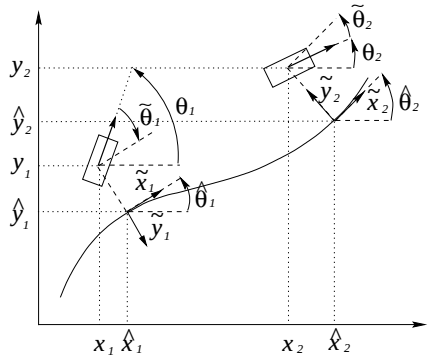

Figure 1: Reference path and transformed coordinates.

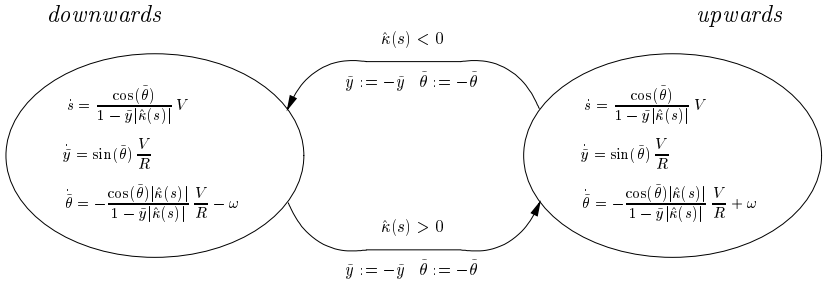

Figure 2: Hybrid automaton $PTHA_{\mathcal{J}}$ modelling the car in the transformed state space.

- the arclength parameter s defines the position of the Frenet's frame along the curve;
- $\tilde{y}$ denotes the position of the car along the principal normal of $\mathcal{S}_T(s)$ (lateral distance) normalized with respect to the minimum turning radius R;
- $\tilde{\theta}$ denotes its orientation with respect to the tangent axis of $\mathcal{S}_T(s)$ (heading angle error), with sign taken according to the local direction of the binormal axis (see Figure 1).

It can be noticed that this coordinate system is similar to the one used by Samson [10], except for the switchings of the Frenet's frame. In fact, a change of curvature along the path produces a jump of the variables $\tilde{y}$ and $\tilde{\theta}$ to the symmetric point with respect to the origin in the $(\tilde{y}, \tilde{\theta})$–plane. The reason for introducing such discontinuity in the model is related to the different behaviours that a vehicle with bounded curvature has when it approaches a reference path. Indeed, the approach is apparently easier if the vehicle and the center of curvature of the path lie on the opposite sides of the curve[3]. This formulation will turn out to be useful in the verification of the proposed path tracking controller.

The motion of the car in the transformed state $(s, \tilde{y}, \tilde{\theta})^T$ can be described by using the formalism of hybrid automata (see [6, 3]). The discrete nature of the model arises from the fact that the Frenet's frame $\mathcal{S}_T(s)$ changes its orientation during the motion, depending on the sign of the curvature $\hat{\kappa}(s)$. The discrete state, referred to as *bin* , models the two possible orientations of the binormal axis of $\mathcal{S}_T(s(t))$ at time t and assumes either the value *upwards* or the value *downwards*. Its initial value is *upwards*, if $\hat{\kappa}(s(0)) > 0$, or *downwards*, if $\hat{\kappa}(s(0)) \leq 0$. The dynamics the continuous states are obtained by simple computations in the new coordinates. The complete (uncontrolled) Path–Tracking Hybrid Automaton, referred to as $PTHA_{\mathcal{J}}$, is thus as depicted in Figure 2.

Notice that, in the transformed state space adopted in this hybrid model, the path tracking problem reduces to that of stabilizing $(\tilde{y}, \tilde{\theta})$ to $(0, 0)$. However, in the dynamics of these two variables there appears the path curvature function $\hat{\kappa}(s)$, which forces the model to include the evolution of the arclength abscissa s.

[3]For instance, if the vehicle is required to approach a circle with curvature $1/R$, then it can approach it only from outside.

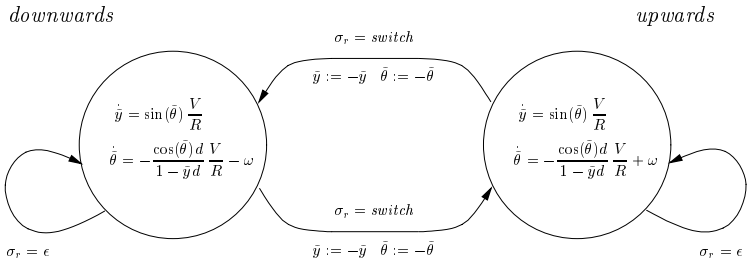

Figure 3: Hybrid automaton $PTHA_{\mathcal{Q}}$ of the vehicle with uncontrollable events (changes of curvature of the tracked path) and a reduced state space.

On the other hand, we should like to design a control law without resorting to the practically unlikely assumption that the path curvature at a generic point on the path is known beforehand or can be measured. We instead assume that only the sign of $\hat{\kappa}(s)$, and not its amplitude, is available to the controller. To model such case, the local curvature $|\hat{\kappa}(s)|$ in the model above is replaced by an unknown but bounded input disturbance $d(t)$ with respect to which the path tracking controller has to be robust. By (3), the disturbance $d(t)$ satisfies

$$0 \leq d(t) \leq C < 1. \tag{5}$$

The path tracking problem can be described in a reduced continuous state space $(\tilde{y}, \tilde{\theta})$. Curvature sign switching conditions $\hat{\kappa}(s) > 0$ and $\hat{\kappa}(s) < 0$ are modelled by a discrete uncontrollable input σ_r, assuming either the value *switch* (when a change of curvature sign occurs) or the *silent move* ϵ (otherwise). The reduced hybrid automaton, referred to as $PTHA_{\mathcal{Q}}$, is reported in Figure 3.

In this case the path tracking problem is formulated as follows:

Problem 1 *Let Γ as in (2) be a feasible reference path. Given the hybrid automaton $PTHA_{\mathcal{Q}}$, find a feedback control law $\omega(bin, (\tilde{y}, \tilde{\theta}))$ satisfying curvature constraint (1) such that, from any initial state $(bin_0, (\tilde{y}_0, \tilde{\theta}_0))$ the trajectory $(\tilde{y}(t), \tilde{\theta}(t))$ converges to the origin under the action of any unknown disturbance $d(t)$, bounded as in (5), and any sequence of uncontrollable events σ_r.*

3 Hybrid path–tracking feedback controller

3.1 Optimal feedback control for line tracking

In [13], the problem of driving a Dubins' car to a straight path has been considered. An optimal feedback control that minimizes the length traveled by the vehicle to reach the specified path was devised. The method is briefly reported in this section to make this paper self-contained and more understandable. Define $\sigma_N(\tilde{y}, \tilde{\theta}) = \tilde{y} + 1 + \cos(\tilde{\theta})$ and $\sigma_P(\tilde{y}, \tilde{\theta}) = \tilde{y} - 1 - \cos(\tilde{\theta})$. The optimal feedback control presented in [13] is defined inside the region

$$\mathcal{D}_{(\tilde{y},\tilde{\theta})} = \begin{cases} (\sigma_N(\tilde{y},\tilde{\theta}) < 0 \ \wedge \ \tilde{\theta} \in [\pi, \frac{3}{2}\pi)\ ) \ \vee \ (\sigma_P(\tilde{y},\tilde{\theta}) \leq 0 \ \wedge \ \tilde{\theta} \in (\frac{\pi}{2}, \pi)\ ) \ \vee \\ (\tilde{\theta} \in [-\frac{\pi}{2}, \frac{\pi}{2}],\ \tilde{y} \in \mathbb{R}) \ \vee \\ (\sigma_N(\tilde{y},\tilde{\theta}) \geq 0 \ \wedge \ \tilde{\theta} \in [-\pi, -\frac{\pi}{2})\ ) \ \vee (\sigma_P(\tilde{y},\tilde{\theta}) > 0 \ \wedge \ \tilde{\theta} \in (-\frac{3}{2}\pi, -\pi)\ ) \end{cases} \tag{6}$$

in the state space $(\tilde{y}, \tilde{\theta})$, which, modulo 2π angles on $\tilde{\theta}$, corresponds to the whole space (see Figure 4). The optimal controller is described by three modes,

$$\begin{array}{ll} \bullet \ \textit{go\_straight}, & \text{where } \omega = 0 \\ \bullet \ \textit{turn\_right}, & \text{where } \omega = -\frac{V}{R} \\ \bullet \ \textit{turn\_left}, & \text{where } \omega = +\frac{V}{R}\ , \end{array} \tag{7}$$

which are chosen as follows

$$[\textit{go\_straight}, \text{if } (\tilde{y}, \tilde{\theta}) \in \Omega^0] \wedge [\textit{turn\_right}, \text{if } (\tilde{y}, \tilde{\theta}) \in \Omega^-] \wedge [\textit{turn\_left}, \text{if } (\tilde{y}, \tilde{\theta}) \in \Omega^+] \tag{8}$$

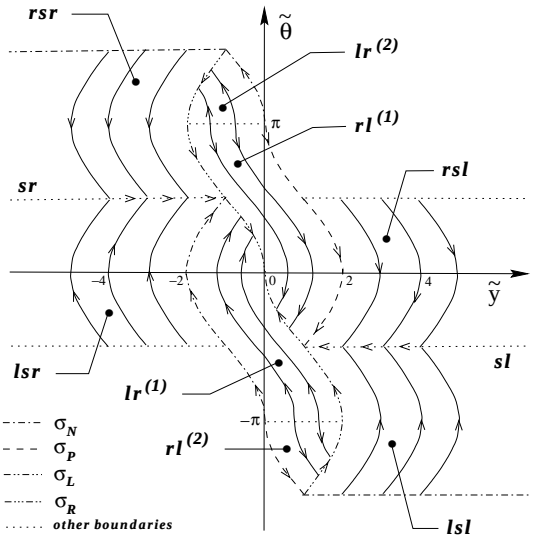

Figure 4: Shortest paths synthesis when $d = 0$.

where the partition $\Omega^0 \cup \Omega^- \cup \Omega^+$ of domain $\mathcal{D}_{(\tilde{y},\tilde{\theta})}$ is defined as in Table 1. In Figure 4 the boundaries between the subsets of the partition $\Omega^0 \cup \Omega^- \cup \Omega^+$ are represented by dotted lines, and the direction of motion, when the reference path is a straight line i.e. $d = 0$, is represented by directed curves.

3.2 Feedback tracking control for generic path

In this section a hybrid feedback controller that solves Problem 1 is derived from the one reported in the previous section. The hybrid model of the vehicle $PTHA_2$ is characterized by the two modes: *upwards* and *downwards*. In mode *downwards* input ω appears with opposite sign with respect to mode *upwards*. Since the controller modes in (8) has been set assuming an upwards binormal axis then, the controller modes *turn_right* and *turn_left* have to be switched when the vehicle is in mode *downwards*. Hence, for a generic feasible path Γ, the full–state feedback controller is defined in $\{upwards, downwards\} \times \mathcal{D}_{(\tilde{y},\tilde{\theta})}$ by setting the controller modes as follows

$$\begin{array}{ll} \bullet\ go\_straight, & \text{if } (bin, (\tilde{y}, \tilde{\theta})) \in \{upwards, downwards\} \times \Omega^0 \\ \bullet\ turn\_right, & \text{if } (bin, (\tilde{y}, \tilde{\theta})) \in (upwards \times \Omega^-) \vee (bin, (\tilde{y}, \tilde{\theta})) \in (downwards \times \Omega^+) \\ \bullet\ turn\_left, & \text{if } (bin, (\tilde{y}, \tilde{\theta})) \in (upwards \times \Omega^+) \vee (bin, (\tilde{y}, \tilde{\theta})) \in (downwards \times \Omega^-) \end{array} \tag{9}$$

where Ω^0, Ω^- and Ω^+ are as in Table 1. The closed–loop hybrid automaton *CLHA* obtained by applying the feedback (7),(9) to the vehicle hybrid automaton $PTHA_2$ is depicted in Figure 5. Since the plant has two modes, namely $\{upwards, downwards\}$, and the controller has three modes, namely $\{go\_straight, turn\_right, turn\_left\}$, then the hybrid closed loop system could have at most six discrete states. However, by carefully analyzing the continuous dynamics of the hybrid automaton $PTHA_2$ depicted in Figures 3 and relations (8) and (9), it is easy to conclude that the following combinations of controller modes and plant modes give rise to the same closed–loop dynamics

- $(go\_straight, upwards)$ and $(go\_straight, downwards\}$
- $(turn\_right, upwards)$ and $(turn\_left, downwards\}$
- $(turn\_left, upwards)$ and $(turn\_right, downwards\}$

Hence, the closed–loop hybrid system *CLHA* has a discrete state *mode* that assumes values in the set $\mathcal{O} = \{zero, negative, positive\}$, as follows

$$\begin{array}{ll} \bullet\ mode = zero & \text{if } (\tilde{y}, \tilde{\theta}) \in \Omega^0 \\ \bullet\ mode = negative & \text{if } (\tilde{y}, \tilde{\theta}) \in \Omega^- \\ \bullet\ mode = positive & \text{if } (\tilde{y}, \tilde{\theta}) \in \Omega^+. \end{array} \tag{10}$$

$\mathbf{O}$	=	$\{(0,0)\}$	$\mathbf{r}^{(1)}$	=	$\{(\tilde{y},\tilde{\theta})\|\tilde{\theta}\in(0,\frac{\pi}{2}),\sigma_R(\tilde{y},\tilde{\theta})=0\}$
			$\mathbf{l}^{(1)}$	=	$\{(\tilde{y},\tilde{\theta})\|\tilde{\theta}\in(-\frac{\pi}{2},0),\sigma_L(\tilde{y},\tilde{\theta})=0\}$
Ω^0	=	$\mathbf{sr}\cup\mathbf{sl}\cup\mathbf{O}$	$\mathbf{r}^{(2)}$	=	$\{(\tilde{y},\tilde{\theta})\|\tilde{\theta}\in[\frac{\pi}{2},\pi),\sigma_R(\tilde{y},\tilde{\theta})=0\}$
Ω^-	=	$\mathbf{r}\cup\mathbf{rsr}\cup\mathbf{rsl}\cup\mathbf{rl}^{(1)}\cup\mathbf{rl}^{(2)}$	$\mathbf{l}^{(2)}$	=	$\{(\tilde{y},\tilde{\theta})\|\tilde{\theta}\in(-\pi,-\frac{\pi}{2}],\sigma_L(\tilde{y},\tilde{\theta})=0\}$
Ω^+	=	$\mathbf{l}\cup\mathbf{lsr}\cup\mathbf{lsl}\cup\mathbf{lr}^{(1)}\cup\mathbf{lr}^{(2)}$	$\mathbf{r}^{(3)}$	=	$\{(\tilde{y},\tilde{\theta})\|\tilde{\theta}\in[\pi,\frac{3}{2}\pi),\sigma_R(\tilde{y},\tilde{\theta})=0\}\cup\{(0,\pi)$
			$\mathbf{l}^{(3)}$	=	$\{(\tilde{y},\tilde{\theta})\|\tilde{\theta}\in(-\frac{3}{2}\pi,-\pi],\sigma_L(\tilde{y},\tilde{\theta})=0\}$
$\mathbf{r}$	=	$\mathbf{r}^{(1)}\cup\mathbf{r}^{(2)}\cup\mathbf{r}^{(3)}$	$\mathbf{lr}^{(1.1)}$	=	$\{(\tilde{y},\tilde{\theta})\|\tilde{\theta}\in(0,\frac{\pi}{2}),\sigma_N(\tilde{y},\tilde{\theta})\geq 0,\sigma_R(\tilde{y},\tilde{\theta})<0\}$
$\mathbf{lr}^{(1)}$	=	$\mathbf{lr}^{(1.1)}\cup\mathbf{lr}^{(1.2)}\cup\mathbf{lr}^{(1.3)}$	$\mathbf{rl}^{(1.1)}$	=	$\{(\tilde{y},\tilde{\theta})\|\tilde{\theta}\in(-\frac{\pi}{2},0),\sigma_L(\tilde{y},\tilde{\theta})>0,\sigma_P(\tilde{y},\tilde{\theta})\leq 0\}$
$\mathbf{lsr}$	=	$\mathbf{lsr}^{(1)}\cup\mathbf{lsr}^{(2)}$	$\mathbf{lr}^{(1.2)}$	=	$\{(\tilde{y},\tilde{\theta})\|\tilde{\theta}\in(-\frac{\pi}{2},0],\sigma_N(\tilde{y},\tilde{\theta})\geq 0,\sigma_L(\tilde{y},\tilde{\theta})<0\}$
$\mathbf{rsr}$	=	$\mathbf{rsr}^{(1)}\cup\mathbf{rsr}^{(2)}$	$\mathbf{rl}^{(1.2)}$	=	$\{(\tilde{y},\tilde{\theta})\|\tilde{\theta}\in[0,\frac{\pi}{2}),\sigma_R(\tilde{y},\tilde{\theta})>0,\sigma_P(\tilde{y},\tilde{\theta})\leq 0\}$
$\mathbf{l}$	=	$\mathbf{l}^{(1)}\cup\mathbf{l}^{(2)}\cup\mathbf{l}^{(3)}$	$\mathbf{lr}^{(1.3)}$	=	$\{(\tilde{y},\tilde{\theta})\|\tilde{\theta}\in(-\pi,-\frac{\pi}{2}],\sigma_N(\tilde{y},\tilde{\theta})\geq 0,\sigma_L(\tilde{y},\tilde{\theta})<0\}$
$\mathbf{rl}^{(1)}$	=	$\mathbf{rl}^{(1.1)}\cup\mathbf{rl}^{(1.2)}\cup\mathbf{rl}^{(1.3)}$	$\mathbf{rl}^{(1.3)}$	=	$\{(\tilde{y},\tilde{\theta})\|\tilde{\theta}\in[\frac{\pi}{2},\pi),\sigma_R(\tilde{y},\tilde{\theta})>0,\sigma_P(\tilde{y},\tilde{\theta})\leq 0\}$
$\mathbf{rsl}$	=	$\mathbf{rsl}^{(1)}\cup\mathbf{rsl}^{(2)}$	$\mathbf{lr}^{(2)}$	=	$\{(\tilde{y},\tilde{\theta})\|\tilde{\theta}\in[\pi,\frac{3}{2}\pi),\sigma_R(\tilde{y},\tilde{\theta})>0,\sigma_N(\tilde{y},\tilde{\theta})<0\}$
$\mathbf{lsl}$	=	$\mathbf{lsl}^{(1)}\cup\mathbf{lsl}^{(2)}$	$\mathbf{rl}^{(2)}$	=	$\{(\tilde{y},\tilde{\theta})\|\tilde{\theta}\in(-\frac{3}{2}\pi,-\pi],\sigma_P(\tilde{y},\tilde{\theta})>0,\sigma_L(\tilde{y},\tilde{\theta})<0\}$
			$\mathbf{sr}$	=	$\{(\tilde{y},\tilde{\theta})\|\tilde{y}<-1,\tilde{\theta}=\frac{\pi}{2}\}$
			$\mathbf{sl}$	=	$\{(\tilde{y},\tilde{\theta})\|\tilde{y}>+1,\tilde{\theta}=-\frac{\pi}{2}\}$
			$\mathbf{lsr}^{(1)}$	=	$\{(\tilde{y},\tilde{\theta})\|\tilde{\theta}\in[0,\frac{\pi}{2}),\sigma_N(\tilde{y},\tilde{\theta})<0\}$
			$\mathbf{rsl}^{(1)}$	=	$\{(\tilde{y},\tilde{\theta})\|\tilde{\theta}\in(-\frac{\pi}{2},0],\sigma_P(\tilde{y},\tilde{\theta})>0\}$
			$\mathbf{lsr}^{(2)}$	=	$\{(\tilde{y},\tilde{\theta})\|\tilde{\theta}\in[-\frac{\pi}{2},0),\sigma_N(\tilde{y},\tilde{\theta})<0\}$
			$\mathbf{rsl}^{(2)}$	=	$\{(\tilde{y},\tilde{\theta})\|\tilde{\theta}\in(0,\frac{\pi}{2}],\sigma_P(\tilde{y},\tilde{\theta})>0\}$
			$\mathbf{rsr}^{(1)}$	=	$\{(\tilde{y},\tilde{\theta})\|\tilde{\theta}\in(\frac{\pi}{2},\pi),\sigma_R(\tilde{y},\tilde{\theta})<0\}$
			$\mathbf{lsl}^{(1)}$	=	$\{(\tilde{y},\tilde{\theta})\|\tilde{\theta}\in(-\pi,-\frac{\pi}{2}),\sigma_L(\tilde{y},\tilde{\theta})>0\}$
			$\mathbf{rsr}^{(2)}$	=	$\{(\tilde{y},\tilde{\theta})\|\tilde{\theta}\in[\pi,\frac{3}{2}\pi),\sigma_R(\tilde{y},\tilde{\theta})<0\}$
			$\mathbf{lsl}^{(2)}$	=	$\{(\tilde{y},\tilde{\theta})\|\tilde{\theta}\in(-\frac{3}{2}\pi,-\pi],\sigma_L(\tilde{y},\tilde{\theta})>0\}$

$$\sigma_N(\tilde{y},\tilde{\theta})=\tilde{y}+1+\cos(\tilde{\theta})$$
$$\sigma_P(\tilde{y},\tilde{\theta})=\tilde{y}-1-\cos(\tilde{\theta})$$
$$\sigma_R(\tilde{y},\tilde{\theta})=\tilde{y}+1-\cos(\tilde{\theta})$$
$$\sigma_L(\tilde{y},\tilde{\theta})=\tilde{y}-1+\cos(\tilde{\theta})$$

Table 1: Partition of domain $\mathcal{D}_{(\tilde{y},\tilde{\theta})}$ used to define the shortest path synthesis.

The initial state $(mode_0,(\tilde{y}_0,\tilde{\theta}_0))$ of the hybrid automaton *CLHA* has to satisfy (10).

The coordinate transformation $(x,y,\theta)\rightarrow(s,\tilde{y},\tilde{\theta})$ becomes singular when the vehicle lies on the center of the local osculating circle to the path Γ. That is if, at some time $\bar{t}$, $\tilde{y}(\bar{t})\,|\hat{\kappa}(s(\bar{t}))|=1$, or equivalently $\tilde{y}(\bar{t})\,d(\bar{t})=1$. For any initial configuration $(M(x_0,y_0),\theta_0)$, with $M(x_0,y_0)\in\mathcal{T}_\Gamma$ as in (4), the corresponding state $(\tilde{y}_0,\tilde{\theta}_0)$ satisfies $\tilde{y}_0<C^{-1}$. Further, since by (5) $d\leq C$, then $\tilde{y}_0\,d<1$ at the given initial condition. However, to ensure that

$$\tilde{y}\,d<1\quad\text{i.e.}\quad 1-\tilde{y}\,d>0 \tag{11}$$

holds along all the trajectories of *CLHA* , we need to further restrict the admissible initial vehicle configurations, in terms of its initial orientation θ_0.

Proposition 1 *Let the continuous disturbance d be bounded to belong to the interval $[0,C]$, with*

$$C<\sqrt{2}-1 \tag{12}$$

Then, (11) is satisfied along all trajectories of CLHA provided that the initial configuration $(mode_0,(\tilde{y}_0,\tilde{\theta}_0))$ is such that

$$(\tilde{y}_0,\tilde{\theta}_0)\in\mathcal{I}_{(\tilde{y},\tilde{\theta})}=\left\{(\tilde{y},\tilde{\theta})\ \in\mathcal{D}_{(\tilde{y},\tilde{\theta})}|\ \sigma_1(\tilde{y},\tilde{\theta})>0\ \ and\ \ \sigma_2(\tilde{y},\tilde{\theta})<0\right\}. \tag{13}$$

where

$$\sigma_1(\tilde{y},\tilde{\theta})=\begin{cases}\tilde{y}+C^{-1} & \text{if }\theta\in[0,\pi]\\ \tilde{y}-(1+C)+C^{-1}+(1+C)\,|\cos(\tilde{\theta})|=0 & \text{if }\theta\in[-\frac{\pi}{2},0)\cup[\pi,\frac{3}{2}\pi)\end{cases}$$

$$\sigma_2(\tilde{y},\tilde{\theta})=\begin{cases}\tilde{y}-C^{-1} & \text{if }\theta\in[-\pi,0]\\ \tilde{y}+(1+C)-C^{-1}-(1+C)\,|\cos(\tilde{\theta})|=0 & \text{if }\theta\in(-\frac{3}{2}\pi,-\pi)\cup(0,\frac{\pi}{2}]\end{cases}$$

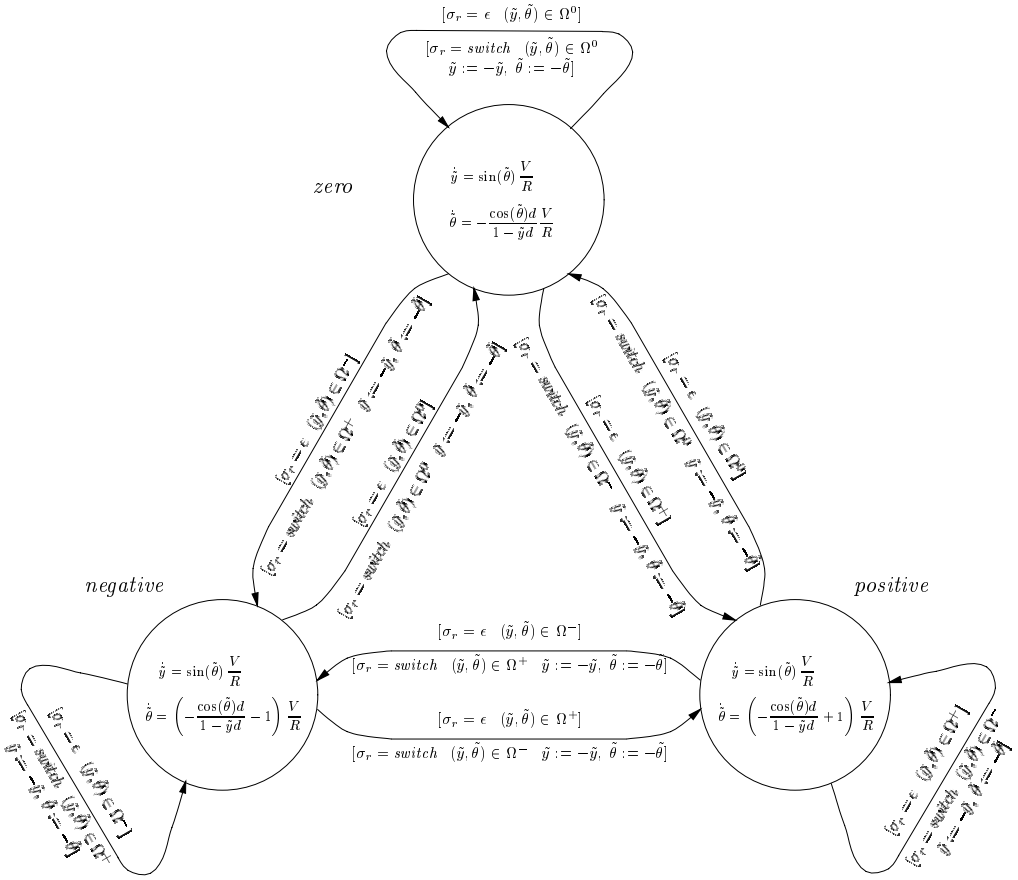

Figure 5: Hybrid model of the closed-loop system *CLHA* .

Proof of Proposition 1. We have to show that the set $\mathcal{I}_{(\tilde{y},\tilde{\theta})}$ in (13) is a robust invariant set, under any action of the continuous disturbance d, bounded by C as in (12), and any action of the discrete disturbance $\sigma_r = switch$. To prove this we will first show that, along the trajectories of the closed–loop hybrid system *CLHA* , $\dot{\sigma}_1 > 0$ in a right neighbourhood of the curve $\sigma_1(\tilde{y},\tilde{\theta}) = 0$, and $\dot{\sigma}_2 < 0$ in a left neighbourhood of the curve $\sigma_2(\tilde{y},\tilde{\theta}) = 0$. The upper bound (12) for C guarantees that there exists a right neighbourhood of the curve $\sigma_1(\tilde{y},\tilde{\theta}) = 0$ contained in the region $\mathbf{rsr} \cup \mathbf{sr} \cup \mathbf{lsr}$, and there exists a left neighbourhood of the curve $\sigma_2(\tilde{y},\tilde{\theta}) = 0$ contained in the region $\mathbf{rsl} \cup \mathbf{sl} \cup \mathbf{lsl}$. This simplifies the analysis of the closed–loop system trajectories.

By (10) and (7), the closed–loop continuous dynamics are

$$\dot{\tilde{y}} = \sin(\tilde{\theta})\,\frac{V}{R} \tag{14}$$

$$\dot{\tilde{\theta}} = \begin{cases} -\frac{\cos(\tilde{\theta})d}{1-\tilde{y}d}\,\frac{V}{R} & \text{if } mode = zero \\ \left(-\frac{\cos(\tilde{\theta})d}{1-\tilde{y}d} - 1\right)\frac{V}{R} & \text{if } mode = negative \\ \left(-\frac{\cos(\tilde{\theta})d}{1-\tilde{y}d} + 1\right)\frac{V}{R} & \text{if } mode = positive \end{cases}$$

Hence, by (14), along the trajectories of the closed–loop hybrid system *CLHA* we have

$$\dot{\sigma}_1|_{(\tilde{y},\tilde{\theta})\in \mathbf{rsr}\cup\mathbf{sr}\cup\mathbf{lsr}} = \begin{cases} \sin(\tilde{\theta})\,\frac{V}{R} & \text{if } \theta \in [0,\pi] \\ \left[1-(1+C)\,\text{sign}(\cos(\tilde{\theta}))\frac{R}{V}\,\dot{\theta}\right]\,\sin(\tilde{\theta})\frac{V}{R} & \text{if } \theta \in [-\frac{\pi}{2},0)\cup[\pi,\frac{3}{2}\pi) \end{cases} \tag{15}$$

and

$$\dot{\sigma}_2|_{(\tilde{y},\tilde{\theta})\in \mathbf{rsl}\cup\mathbf{sl}\cup\mathbf{lsl}} = \begin{cases} \sin(\tilde{\theta})\,\frac{V}{R} & \text{if } \theta \in [-\pi,0] \\ \left[1+(1+C)\,\text{sign}(\cos(\tilde{\theta}))\frac{R}{V}\,\dot{\theta}\right]\,\sin(\tilde{\theta})\frac{V}{R} & \text{if } \theta \in [-\frac{3}{2}\pi,-\pi)\cup(0,\frac{\pi}{2}) \end{cases} \tag{16}$$

Furthermore, for $(\tilde{y},\tilde{\theta}) \in \mathbf{rsr}\cup\mathbf{lsr}$, since, by Table 1 $\tilde{y} < -1$, then by (11), $\frac{1-\tilde{y}d}{d} = \frac{1}{d} - \tilde{y} > \frac{1}{C} + 1$ and $\frac{d}{1-\tilde{y}d} < \frac{C}{1+C}$. Hence, by (14), we have

$$\begin{array}{rcll} \frac{R}{V}\,\dot{\tilde{\theta}} & < & -\cos(\tilde{\theta})\frac{C}{1+C} - 1 \le -\frac{1}{1+C} & \text{for } (\tilde{y},\tilde{\theta}) \in \mathbf{rsr} \subset \Omega^- \text{ where } \cos(\tilde{\theta}) \le 0 \\ \frac{R}{V}\,\dot{\tilde{\theta}} & > & -\cos(\tilde{\theta})\frac{C}{1+C} + 1 \ge +\frac{1}{1+C} & \text{for } (\tilde{y},\tilde{\theta}) \in \mathbf{lsr} \subset \Omega^+ \text{ where } \cos(\tilde{\theta}) \ge 0 \\ \frac{R}{V}\,\dot{\tilde{\theta}} & < & -\cos(\tilde{\theta})\,\frac{d}{1-\tilde{y}d} - 1 \le -1 & \text{for } (\tilde{y},\tilde{\theta}) \in \mathbf{rsl} \subset \Omega^- \text{ where } \cos(\tilde{\theta}) \ge 0 \\ \frac{R}{V}\,\dot{\tilde{\theta}} & > & -\cos(\tilde{\theta})\,\frac{d}{1-\tilde{y}d} + 1 \ge +1 & \text{for } (\tilde{y},\tilde{\theta}) \in \mathbf{lsl} \subset \Omega^+ \text{ where } \cos(\tilde{\theta}) \le 0 \end{array}$$

From (15–16) and the above upper and lower bounds on $\dot{\tilde{\theta}}$ we can conclude that in a right neighbourhood of the curve $\sigma_1(\tilde{y},\tilde{\theta}) = 0$, contained in $\mathbf{rsr}\cup\mathbf{sr}\cup\mathbf{lsr}$, we have $\dot{\sigma}_1 > 0$, and in a left neighbourhood of the curve $\sigma_2(\tilde{y},\tilde{\theta}) = 0$, contained in $\mathbf{rsl}\cup\mathbf{sl}\cup\mathbf{lsl}$, we have $\dot{\sigma}_2 < 0$. Finally, since under the action of the discrete disturbance $\sigma_r = \textit{switch}$ the continuous state is reset to the symmetric point with respect to the origin, at which corresponds a same value of functions $\sigma_i(\tilde{y},\tilde{\theta})$, invariance the set $\mathcal{I}_{(\tilde{y},\tilde{\theta})}$ is preserved under any switchings of the Frenet frame.

Remark 1 *Relaxing condition $C < \sqrt{2}-1$ to $C < \frac{1}{3}$, an easier proof could be obtained of the same result (see [4]).*

In Figure 6, the boundary curves $\sigma_1(\tilde{y},\tilde{\theta}) = 0$ and $\sigma_2(\tilde{y},\tilde{\theta}) = 0$ are reported for $C = \sqrt{2}-1$ and $C = 1/4$. Notice that curve $\sigma_1(\tilde{y},\tilde{\theta}) = 0$ passes through the points $(-C^{-1}+1+C, -\frac{\pi}{2})$, $(-C^{-1}, 0)$, $(-C^{-1}, \pi)$, $(-C^{-1}+1+C, \frac{3}{2}\pi)$, while the curve $\sigma_2(\tilde{y},\tilde{\theta}) = 0$ passes through the points $(C^{-1}-1-C, -\frac{3}{2}\pi)$, $(C^{-1}, -\pi)$, $(C^{-1}, 0)$, $(C^{-1}-1-C, \frac{\pi}{2})$. In particular, for $C \longrightarrow \sqrt{2}-1$, the curve $\sigma_1(\tilde{y},\tilde{\theta}) = 0$ passes through the points $(-1, -\frac{\pi}{2})$ and $(-1, \frac{3}{2}\pi)$, while the curve $\sigma_2(\tilde{y},\tilde{\theta}) = 0$ passes through the points $(+1, -\frac{3}{2}\pi)$ and $(+1, \frac{\pi}{2})$. Moreover, for any configuration $(\tilde{y},\tilde{\theta})$ in the set $\mathcal{I}_{(\tilde{y},\tilde{\theta})}$ condition (11) is satisfied when d belongs to the interval $[0, C]$.

Note that, for initial configurations satisfying (13) we have $M(x_0, y_0) \in \mathcal{T}_\Gamma$ as in (4). By Proposition 1, if a reference path Γ has minimum radius of curvature R_Γ greater than twice the minimum turning radius R of the vehicle, then for any initial configuration $(M(x_0, y_0), \theta_0)$, with lateral position and orientation errors bounded to belong to $\mathcal{I}_{(\tilde{y},\tilde{\theta})}$ as in (13), condition (11) is ensured.

4 Verification of the hybrid path–tracking controller

In this section the behaviour of the hybrid automaton *CLHA* is analyzed by introducing an equivalence relation $\sim$ in the hybrid state space $\mathcal{O}\times\mathcal{D}_{(\tilde{y},\tilde{\theta})}$ and by computing the corresponding quotient system (see [6]).

Consider the partition $\Pi_{(\tilde{y},\tilde{\theta})}$ of the domain $\mathcal{D}_{(\tilde{y},\tilde{\theta})}$ in (6) given by the 24 subsets

$$\left\{\mathbf{r}^{(1)}, \cdots, \mathbf{rl}^{(2)}\mathbf{l}^{(3)}, \cdots, \mathbf{lsl}^{(2)}, \mathbf{O}\right\},$$

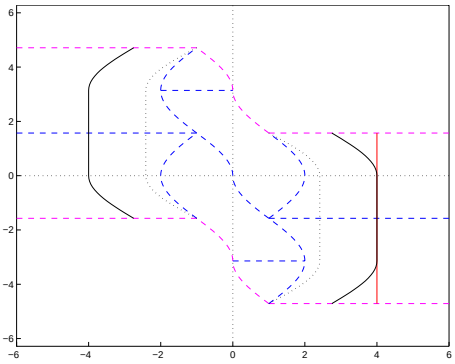

Figure 6: Curve $\sigma_1(\tilde{y},\tilde{\theta})=0$ (for negative $\tilde{y}$) and curve $\sigma_2(\tilde{y},\tilde{\theta})=0$ (for positive $\tilde{y}$), when $C=\sqrt{2}-1$ (dotted line) and $C=1/4$ (solid line).

defined in Table 1, with $\mathbf{rl}^{(2)}$ and $\mathbf{l}^{(3)}$ replaced by $\mathbf{rl}^{(2)}\mathbf{l}^{(3)}$. We say that $(mode_1,(\tilde{y}_1,\tilde{\theta}_1))$, $(mode_2,(\tilde{y}_2,\tilde{\theta}_2))$ are equivalent, i.e. $(mode_1,(\tilde{y}_1,\tilde{\theta}_1))\sim(mode_2,(\tilde{y}_2,\tilde{\theta}_2))$, iff $(\tilde{y}_1,\tilde{\theta}_1)$ and $(\tilde{y}_2,\tilde{\theta}_2)$ belong to the same subset $\mathbf{p}\in\Pi_{(\tilde{y},\tilde{\theta})}$. We associate to the corresponding quotient space $Q^{\sim}=\left\{\mathcal{O}\times\mathbf{r}^{(1)},\cdots,\mathcal{O}\times\mathbf{O}\right\}$ a nonderministic finite state machine, referred to as FSM_{PTC} , whose states correspond to the equivalence classes in $Q^{\sim}$ (labeled, with a slight abuse of notation, $\mathbf{r}^{(1)},\cdots,\mathbf{O}$). The next–state function of FSM_{PTC} is defined as follows: for any $Q_1,Q_2\in Q^{\sim}$, a transition from Q_1 to Q_2 occurs iff there exists an arc of trajectory of the hybrid automaton $CLHA$ from some $(mode_1,(\tilde{y}_1,\tilde{\theta}_1))\in Q_1$ to some $(mode_2,(\tilde{y}_2,\tilde{\theta}_2))\in Q_2$, for some discrete disturbance σ_r and some continuous disturbance d.

Proposition 2 *Given the hybrid system CLHA , if the discrete disturbance σ_r always takes the value ϵ, then, for any initial hybrid state $(mode,(\tilde{y}_0,\tilde{\theta}_0))\in\mathcal{O}\times\mathcal{I}_{(\tilde{y},\tilde{\theta})}$ as in (13), under the action of any disturbance d bounded as in (5) with C as in (12), we have:*

- *the quotient system obtained from the equivalence relation $\sim$ is the finite state machine FSM_{PTC} depicted in Figure 8;*
- *an upper bound for the space traveled by the origin of the Frenet's frame along the path Γ, when the hybrid state is in a given equivalence class is represented by the weight associated to the exiting arc;*
- *the quotient system FSM_{PTC} remains in each equivalence class a bounded amount of time, except for the equivalent class $\mathbf{O}$ where $(\tilde{y},\tilde{\theta})=(0,0)$.*

Proof of Proposition 2. In this proof we show that the finite state machine FSM_{PTC} , which abstracts the behaviour of the closed–loop hybrid system $CLHA$, is as reported in Figure 8. Further, we provide upper bounds for the time spent by FSM_{PTC} in each state and upper bounds for the length of the corresponding arc of the reference path Γ spanned by the origin of the Frenet frame. In the following, unless differently specified, we assume, according to (12), $C<0.5$, so that, by Proposition 1, condition (11) is guaranteed along hybrid system trajectories.

Introduce

$$\sigma_N(\tilde{y},\tilde{\theta}) = \tilde{y}+1+\cos(\tilde{\theta}), \tag{17}$$
$$\sigma_P(\tilde{y},\tilde{\theta}) = \tilde{y}-1-\cos(\tilde{\theta}). \tag{18}$$
$$\sigma_R(\tilde{y},\tilde{\theta}) = \tilde{y}+1-\cos(\tilde{\theta}), \tag{19}$$
$$\sigma_L(\tilde{y},\tilde{\theta}) = \tilde{y}-1+\cos(\tilde{\theta}). \tag{20}$$

We'll make use of the derivatives with respect to time of σ_P, σ_R, σ_N and σ_L, as defined in (18), (19), (17)

and (20), respectively. Under feedback (9), we have

$$\dot{\sigma}_P = \dot{\sigma}_R = \begin{cases} -\sin(\tilde{\theta})\frac{\cos(\tilde{\theta})d}{1-\tilde{y}d}\frac{V}{R} \\ \quad \text{in mode } \textit{negative} \\ \sin(\tilde{\theta})\left[-\frac{\cos(\tilde{\theta})d}{1-\tilde{y}d}+2\right]\frac{V}{R} \\ \quad \text{in mode } \textit{positive} \end{cases} \tag{21}$$

and

$$\dot{\sigma}_N = \dot{\sigma}_L = \begin{cases} \sin(\tilde{\theta})\left[\frac{\cos(\tilde{\theta})d}{1-\tilde{y}d}+2\right]\frac{V}{R} \\ \quad \text{in mode } \textit{negative} \\ \sin(\tilde{\theta})\frac{\cos(\tilde{\theta})d}{1-\tilde{y}d}\frac{V}{R} \\ \quad \text{in mode } \textit{positive} \end{cases} \tag{22}$$

In the sequel, the behaviour of the closed-loop hybrid system *CLHA* in each region of the continuous state space partition defined in Table 1 is discussed.

Regions $\mathbf{rsr}^{(1)}$ and $\mathbf{rsr}^{(2)}$. The system mode is *negative*. By Table 1, $\tilde{y} < -1$ and $\cos(\tilde{\theta}) < 0$. Further, by (11), $\frac{1-\tilde{y}d}{d} = \frac{1}{d} - \tilde{y} > 2$. Then, $0 \leq \frac{-\cos(\tilde{\theta})d}{1-\tilde{y}d} < \frac{-\cos(\tilde{\theta})}{2} < \frac{1}{2}$ (where equality holds for $d = 0$) and $\frac{-\cos(\tilde{\theta})d}{1-\tilde{y}d} - 1 < -\frac{1}{2}$. Hence, by (14), $\dot{\tilde{\theta}} < -\frac{1}{2}\frac{V}{R}$. Therefore, the continuous state $(\tilde{y}, \tilde{\theta})$

- cannot exit boundary $\tilde{\theta} = \frac{3}{2}\pi$ and enter $\mathbf{lsr}^{(2)}$;
- may leave $\mathbf{rsr}^{(2)}$ to enter $\mathbf{rsr}^{(1)}$;
- may leave $\mathbf{rsr}^{(1)}$ to enter $\mathbf{sr}$.

Furthermore, by (21), if $d = 0$ then $\dot{\sigma}_R = 0$ and trajectories are parallel to $\mathbf{r}$. While, if $d > 0$, then $\dot{\sigma}_R < 0$, for $\tilde{\theta} \in (\pi, \frac{3}{2}\pi)$, and $\dot{\sigma}_R > 0$, for $\tilde{\theta} \in (\frac{\pi}{2}, \pi)$. Therefore, $(\tilde{y}, \tilde{\theta})$

- neither reaches nor exits from $\mathbf{r}^{(3)} \cup \mathbf{r}^{(2)}$, if $d = 0$;
- leaves $\mathbf{r}^{(3)}$ to enter $\mathbf{rsr}^{(2)}$, if $d > 0$;
- may leave $\mathbf{rsr}^{(1)}$ to enter $\mathbf{r}^{(2)}$, if $d > 0$.

Regions $\mathbf{lsr}^{(1)}$ and $\mathbf{lsr}^{(2)}$. The system mode is *positive*. By Table 1, $\tilde{y} < -1$ and $\cos(\tilde{\theta}) \geq 0$. Further, by (11), $\frac{1-\tilde{y}d}{d} = \frac{1}{d} - \tilde{y} > 2$ Then, $0 \leq \frac{\cos(\tilde{\theta})d}{1-\tilde{y}d} < \frac{\cos(\tilde{\theta})}{2} < \frac{1}{2}$ (where equality holds for $d = 0$ or $\tilde{\theta} = -\frac{\pi}{2}$) and $-\frac{\cos(\tilde{\theta})d}{1-\tilde{y}d} + 1 > \frac{1}{2}$. Hence, by (14), $\dot{\tilde{\theta}} > \frac{1}{2}\frac{V}{R}$. Therefore, the continuous state $(\tilde{y}, \tilde{\theta})$

- cannot exit the boundary $\tilde{\theta} = -\frac{\pi}{2}$ and enter $\mathbf{rsr}^{(2)}$;
- may leave $\mathbf{lsr}^{(2)}$ to enter $\mathbf{lsr}^{(1)}$;
- may leave $\mathbf{lsr}^{(1)}$ to enter $\mathbf{sr}$.

Furthermore, by (22), if $d = 0$ then $\dot{\sigma}_N = 0$ and the trajectories are parallel to curve $\sigma_N(\tilde{y}, \tilde{\theta}) = 0$. While, if $d > 0$, then $\dot{\sigma}_N > 0$, for $\tilde{\theta} \in (0, \frac{\pi}{2})$, and $\dot{\sigma}_N < 0$, for $\tilde{\theta} \in (-\frac{\pi}{2}, 0)$. Then, $(\tilde{y}, \tilde{\theta})$

- neither reaches nor exits from $\mathbf{lr}^{(1.2)} \cup \mathbf{lr}^{(1.1)}$, if $d = 0$;
- leaves $\mathbf{lr}^{(1.2)}$ to enter $\mathbf{lsr}^{(2)}$, if $d > 0$;
- may leave $\mathbf{lsr}^{(1)}$ to enter $\mathbf{lr}^{(1.1)}$, if $d > 0$.

Regions $\mathbf{rsl}^{(1)}$ and $\mathbf{rsl}^{(2)}$. The system mode is *negative*. By Table 1, $\cos(\tilde{\theta}) \geq 0$. Assuming (11), $\frac{\cos(\tilde{\theta})d}{1-\tilde{y}d} \geq 0$ (where equality holds for $d = 0$ or $\tilde{\theta} = \frac{\pi}{2}$) and $-\frac{\cos(\tilde{\theta})d}{1-\tilde{y}d} - 1 \leq -1$. Then, by (14), $\dot{\tilde{\theta}} \leq -\frac{V}{R}$. Therefore, the continuous state $(\tilde{y}, \tilde{\theta})$

- cannot exit boundary $\tilde{\theta} = \frac{\pi}{2}$ and enter $\mathbf{lsl}^{(2)}$;
- may leave $\mathbf{rsl}^{(2)}$ to enter $\mathbf{rsl}^{(1)}$;
- may leave $\mathbf{rsl}^{(1)}$ to enter $\mathbf{sl}$.

Furthermore, by (21), if $d = 0$ then $\dot{\sigma}_P = 0$ and trajectories are parallel to $\sigma_P(\tilde{y}, \tilde{\theta}) = 0$. While, if $d > 0$, then $\dot{\sigma}_P < 0$, for $\tilde{\theta} \in (0, \frac{\pi}{2})$, and $\dot{\sigma}_P > 0$, for $\tilde{\theta} \in (-\frac{\pi}{2}, 0)$. Therefore, $(\tilde{y}, \tilde{\theta})$

- neither reaches nor exits from $\mathbf{rl}^{(1.1)} \cup \mathbf{rl}^{(1.2)}$, if $d = 0$;
- may leave $\mathbf{rsl}^{(2)}$ to enter $\mathbf{rl}^{(1.2)}$, if $d > 0$;
- may leave $\mathbf{rl}^{(1.1)}$ to enter $\mathbf{rsl}^{(1)}$, if $d > 0$.

Regions $\mathbf{lsl}^{(1)}$ and $\mathbf{lsl}^{(2)}$. The system mode is *positive*. By Table 1, $\cos(\tilde{\theta}) < 0$. Assuming (11), $-\frac{\cos(\tilde{\theta})d}{1-\tilde{y}d} \geq 0$ (where equality holds for $d = 0$) and $-\frac{\cos(\tilde{\theta})d}{1-\tilde{y}d} + 1 \geq 1$. Then, by (14), $\dot{\tilde{\theta}} \geq \frac{V}{R}$. Therefore, the continuous state $(\tilde{y}, \tilde{\theta})$

- cannot exit boundary $\tilde{\theta} = -\frac{3}{2}\pi$ and enter $\mathbf{rsl}^{(2)}$;
- may leave $\mathbf{lsl}^{(2)}$ to enter $\mathbf{lsl}^{(1)}$;
- may leave $\mathbf{lsl}^{(1)}$ to enter $\mathbf{sl}$.

Furthermore, by (22), if $d = 0$ then $\dot{\sigma}_L = 0$ and the trajectories are parallel to $\mathbf{l}$. While, if $d > 0$, then by (22), $\dot{\sigma}_L > 0$, for $\tilde{\theta} \in (-\pi, -\frac{\pi}{2})$, and $\dot{\sigma}_L < 0$, for $\tilde{\theta} \in (-\frac{3}{2}\pi, -\pi)$. Therefore, $(\tilde{y}, \tilde{\theta})$

- neither reaches nor exits from $\mathbf{l}^{(3)} \cup \mathbf{l}^{(2)}$, if $d = 0$;
- leaves $\mathbf{l}^{(2)}$ to enter $\mathbf{lsl}^{(1)}$, if $d > 0$;
- may leave $\mathbf{lsl}^{(2)}$ to enter $\mathbf{l}^{(3)}$, if $d > 0$.

Regions $\mathbf{rl}^{(1.1)}$, $\mathbf{rl}^{(1.2)}$, and $\mathbf{rl}^{(1.3)}$. The system mode is *negative*. By Table 1, $\sigma_P(\tilde{y}, \tilde{\theta}) \leq 0$ which, by (11), implies $\tilde{y} - \frac{1}{d} - \cos(\tilde{\theta}) \leq \tilde{y} - 1 - \cos(\tilde{\theta}) \leq 0$. Assuming (11), one gets $-\frac{\cos(\tilde{\theta})d}{1-\tilde{y}d} - 1 \leq 0$, where equality holds if $d = 1$ and $\sigma_P(\tilde{y}, \tilde{\theta}) = 0$. Therefore, by (14) and (12), $\dot{\tilde{\theta}} < 0$. Furthermore, by (21), if $d = 0$ then $\dot{\sigma}_R = \dot{\sigma}_P = 0$ and the trajectories are parallel to $\mathbf{r}$. While, if $d > 0$, then by (21), $\dot{\sigma}_R = \dot{\sigma}_P > 0$, for $\tilde{\theta} \in (\frac{\pi}{2}, \pi)$, and $\dot{\sigma}_R = \dot{\sigma}_P < 0$, for $\tilde{\theta} \in (0, \frac{\pi}{2})$. Finally, by (22) and (21), $\dot{\sigma}_L < 0$ and $\dot{\sigma}_P > 0$, for $\tilde{\theta} \in (-\frac{\pi}{2}, 0)$. Therefore, the continuous state $(\tilde{y}, \tilde{\theta})$

- cannot exit $\mathbf{rl}^{(1.3)}$ through the boundary $\tilde{y} \in (-2, 0), \tilde{\theta} = \pi$;
- may leave $\mathbf{rl}^{(1.3)}$ to enter $\mathbf{rl}^{(1.2)}$, $\mathbf{rl}^{(1.2)}$ to enter $\mathbf{rl}^{(1.1)}$, and $\mathbf{rl}^{(1.1)}$ and enter $\mathbf{l}^{(1)}$;
- neither reaches nor exits from $\mathbf{r}^{(2)} \cup \mathbf{r}^{(1)} \cup \mathbf{rl}^{(2)} \cup \mathbf{rsl}^{(1)} \cup \mathbf{rsl}^{(2)}$, if $d = 0$;
- leaves $\mathbf{r}^{(2)}$ to enter $\mathbf{rl}^{(1.3)}$ and may leave $\mathbf{rl}^{(1.3)}$ to enter $\mathbf{rl}^{(2)}\mathbf{l}^{(3)}$, if $d > 0$;
- may leave $\mathbf{rsl}^{(2)}$ to enter $\mathbf{rl}^{(1.2)}$ and may leave $\mathbf{rl}^{(1.2)}$ to enter $\mathbf{r}^{(1)}$, if $d > 0$;
- may leave $\mathbf{rl}^{(1.1)}$ to enter $\mathbf{rsl}^{(1)}$, if $d > 0$.

Regions $\mathbf{lr}^{(1.1)}$, $\mathbf{lr}^{(1.2)}$ and $\mathbf{lr}^{(1.3)}$. The system mode is *positive*. By Table 1, $\sigma_L(\tilde{y}, \tilde{\theta}) < 0$ which, by (11), implies $\frac{1}{d} - \tilde{y} - \cos(\tilde{\theta}) \geq 1 - \tilde{y} - \cos(\tilde{\theta}) > 0$. Assuming (11), it gives $-\frac{\cos(\tilde{\theta})d}{1-\tilde{y}d} + 1 > 0$. Hence, by (14), $\dot{\tilde{\theta}} > 0$. Furthermore, by (22), if $d = 0$ then $\dot{\sigma}_L = \dot{\sigma}_N = 0$ and the trajectories are parallel to $\mathbf{l}$. While, if $d > 0$, then by (22), $\dot{\sigma}_L = \dot{\sigma}_N > 0$, for $\tilde{\theta} \in (-\pi, -\frac{\pi}{2})$, and $\dot{\sigma}_L = \dot{\sigma}_N < 0$, for $\tilde{\theta} \in (-\frac{\pi}{2}, 0)$. Finally, by (22) and (21), $\dot{\sigma}_L > 0$ and $\dot{\sigma}_P < 0$, for $\tilde{\theta} \in (0, \frac{\pi}{2})$. Therefore, the continuous state $(\tilde{y}, \tilde{\theta})$

- may leave[4] $\mathbf{lr}^{(1.3)}$ to enter $\mathbf{lr}^{(1.2)}$, $\mathbf{lr}^{(1.2)}$ to enter $\mathbf{lr}^{(1.1)}$, and $\mathbf{lr}^{(1.1)}$ and enter $\mathbf{r}^{(1)}$;

- neither reaches nor exits from $\mathbf{l}^{(2)} \cup \mathbf{l}^{(1)} \cup \mathbf{rl}^{(2)} \cup \mathbf{lsr}^{(1)} \cup \mathbf{lsr}^{(2)}$, if $d = 0$;
- may leave $\mathbf{lr}^{(2)}$ to enter $\mathbf{lr}^{(1.3)}$ and may leave $\mathbf{lr}^{(1.3)}$ to enter $\mathbf{l}^{(2)}$, if $d > 0$;
- leaves $\mathbf{l}^{(1)}$ to enter $\mathbf{lr}^{(1.2)}$ and may leave $\mathbf{lr}^{(1.2)}$ to enter $\mathbf{lsr}^{(2)}$, if $d > 0$;
- may exit $\mathbf{lsr}^{(1)}$ to enter $\mathbf{lr}^{(1.1)}$, if $d > 0$.

Region $\mathbf{lr}^{(2)}$. The system mode is *positive*. By Table 1, $\tilde{y} < 0$ and $\cos(\tilde{\theta}) < 0$. Then, by (11), $1 - \tilde{y}d \geq 1$ and $\frac{-\cos(\tilde{\theta})d}{1-\tilde{y}d} \geq 0$ (where equality holds for $d = 0$) and $\frac{-\cos(\tilde{\theta})d}{1-\tilde{y}d} + 1 \geq 1$. Hence, by (14), $\dot{\tilde{\theta}} \geq \frac{V}{R}$. Furthermore, if $d = 0$, by (22), $\dot{\sigma}_N = 0$ and the trajectories are parallel to $\sigma_N(\tilde{y}, \tilde{\theta}) = 0$. While, if $d > 0$, by (22) and (21), $\dot{\sigma}_R < 0$ and $\dot{\sigma}_N > 0$. Therefore, the continuous state $(\tilde{y}, \tilde{\theta})$

- cannot exit $\mathbf{lr}^{(2)}$ through the boundary $\tilde{y} \in (-2, 0), \tilde{\theta} = \pi$;
- may leave $\mathbf{lr}^{(2)}$ to enter $\mathbf{r}^{(3)}$;
- may leave $\mathbf{lr}^{(2)}$ to enter $\mathbf{lr}^{(1.3)}$, if $d > 0$.

Region $\mathbf{rl}^{(2)}$. The system mode is *negative*. By Table 1, $0 < \tilde{y} < 2$, $\sin(\tilde{\theta}) > 0$ and $\cos(\tilde{\theta}) < 0$. If $d = 0$, by (14), $\dot{\tilde{\theta}} = -\frac{V}{R} < 0$. Otherwise, if $d > 0$, by (14), we have $\dot{\tilde{\theta}} = \frac{\tilde{y}d-1-\cos(\tilde{\theta})d}{1-\tilde{y}d}\frac{V}{R}$. Introducing

$$\phi_d(\tilde{y}, \tilde{\theta}) = \tilde{y}d - 1 - \cos(\tilde{\theta})d, \tag{23}$$

under assumption (11), we have $\dot{\tilde{\theta}} < 0$ $(= 0, > 0)$ if and only if $\phi_d(\tilde{y}, \tilde{\theta}) < 0$ $(= 0, > 0$, resp.). In particular,

1. if $d \leq \frac{1}{3}$, then $\phi_d(\tilde{y}, \tilde{\theta}) \leq \frac{\tilde{y}}{3} - 1 - \frac{\cos(\tilde{\theta})}{3} < 0$, for all $(\tilde{y}, \tilde{\theta})$ in region $\mathbf{rl}^{(2)}$ (being $\phi_d(\tilde{y}, \tilde{\theta}) = 0$ for $d = 3$ and $(\tilde{y}, \tilde{\theta}) \to (2, -\pi)$). Therefore, $\dot{\tilde{\theta}} < 0$ in $\mathbf{rl}^{(2)}$.
2. if $d > \frac{1}{3}$, on the boundary $\tilde{\theta} = -\pi$ we have $\phi_d(\tilde{y}, -\pi) = \tilde{y}d - 1 + d \leq 0$ iff $\tilde{y} \leq \frac{1}{d} - 1$. Then, $\dot{\tilde{\theta}} < 0$ for $\tilde{\theta} = -\pi$ if and only if $\tilde{y} < \frac{1-d}{d}$. Hence, points $(\tilde{y}, \tilde{\theta})$ on the boundary $\tilde{y} \in (0, 2), \tilde{\theta} = -\pi$ are steered to the interior of $\mathbf{rl}^{(2)}$, if $\tilde{y} \in (0, \frac{1-d}{d})$, while are steered to the interior of $\mathbf{lr}^{(1.3)}$ if $\tilde{y} \in (\frac{1-d}{d}, 2)$.

Hence,

- if $d = 0$, by (21), $\dot{\sigma}_P = 0$, hence, the trajectories are parallel to $\sigma_P(\tilde{y}, \tilde{\theta}) = 0$ and exit $\mathbf{rl}^{(2)}$ to enter $\mathbf{l}^{(3)}$;
- if $d \in (0, \frac{1}{3}]$, then $\dot{\tilde{\theta}} < 0$ and, by (21), $\dot{\sigma}_P > 0$. Moreover, since $\frac{1}{d} - \tilde{y} > 1$ then $2(\frac{1}{d} - \tilde{y}) + \cos(\tilde{\theta}) > 1$ and, by (22), $\dot{\sigma}_L > 0$. Therefore, points $(\tilde{y}, \tilde{\theta})$
  - on the boundary $\tilde{y} \in (0, 2), \tilde{\theta} = -\pi$ are steered to the interior of $\mathbf{rl}^{(2)}$;
  - may leave $\mathbf{rl}^{(1.3)}$ to enter $\mathbf{rl}^{(2)}$;
  - leave $\mathbf{rl}^{(2)}$ to enter $\mathbf{l}^{(3)}$.
- if $d \in (\frac{1}{3}, \frac{2}{5}]$, then $\dot{\tilde{\theta}} < 0$ for $\tilde{\theta} = -\pi$ if and only if $\tilde{y} < \frac{1-d}{d}$. Further, by (21), $\dot{\sigma}_P > 0$. Moreover, since $\frac{1}{d} - \tilde{y} > \frac{1}{2}$, then $2(\frac{1}{d} - \tilde{y}) + \cos(\tilde{\theta}) > 0$ and, by (22), $\dot{\sigma}_L > 0$. Therefore, some trajectories
  - may leave $\mathbf{lr}^{(1.3)}$ to enter $\mathbf{rl}^{(2)}$ (crossing the boundary $\tilde{\theta} = -\pi$ at some point with $\tilde{y} \in (0, \frac{1-d}{d})$);
  - may leave $\mathbf{rl}^{(2)}$ to enter $\mathbf{lr}^{(1.3)}$ (crossing the boundary $\tilde{\theta} = -\pi$ at some point with $\tilde{y} \in (\frac{1-d}{d}, 2)$);
  - may leave $\mathbf{rl}^{(2)}$ to enter $\mathbf{l}^{(3)}$.
- if $d \in (\frac{2}{5}, 1]$, as above, $\dot{\tilde{\theta}} < 0$ for $\tilde{\theta} = -\pi$, iff $\tilde{y} < \frac{1-d}{d}$. Further, by (21), $\dot{\sigma}_P > 0$. Moreover, along the curve $\mathbf{l}$, by Table 1 and (22), we have $\dot{\sigma}_L > 0$ if and only if $\tilde{y} \in (0, \frac{d+2}{3d})$. Therefore, some trajectories

[4]The boundary $\tilde{y} \in (0, 2), \tilde{\theta} = -\pi$ is discussed in the analysis of region $\mathbf{rl}^{(2)}$ below.

– may leave $\mathbf{lr}^{(1.3)}$ to enter $\mathbf{rl}^{(2)}$, crossing the boundary at some point with $\tilde{y} \in (0, \frac{1-d}{d})$;

– may leave $\mathbf{rl}^{(2)}$ to enter $\mathbf{lr}^{(1.3)}$, crossing the boundary at some point with $\tilde{y} \in (\frac{1-d}{d}, 2)$;

– may leave $\mathbf{rl}^{(2)}$ to enter $\mathbf{l}^{(3)}$, crossing the boundary at some point with $\tilde{y} \in (1, \frac{d+2}{3d})$;

– may leave $\mathbf{l}^{(3)}$ to enter $\mathbf{rl}^{(2)}$, crossing the boundary at some point with $\tilde{y} \in (\frac{d+2}{3d}, 2)$.

Region sr. The results on region $\mathbf{rsr}^{(1)}$ and $\mathbf{lsr}^{(1)}$ show that $(\tilde{\theta} - \frac{\pi}{2})\dot{\tilde{\theta}} < -\frac{1}{2}\frac{V}{R}$. Therefore, the half line **sr** is attractive from both sides and in the closed loop system a sliding motion is enforced on **sr**, for any disturbance $d(t)$ as in (5). By (14), $\dot{\tilde{y}} = \frac{V}{R}$.

Region sl. Assuming (11), the results on region $\mathbf{rsl}^{(1)}$ and $\mathbf{lsl}^{(1)}$ show that $(\tilde{\theta} + \frac{\pi}{2})\dot{\tilde{\theta}} < -\frac{V}{R}$. Therefore, the half-line **sl** is attractive from both sides and in the closed loop system a sliding motion is enforced on **sl**, for any disturbance $d(t)$ as in (5). By (14), $\dot{\tilde{y}} = -\frac{V}{R}$.

Region $\mathbf{r}^{(1)}$. Curve $\mathbf{r}^{(1)}$ is on the boundary of $\mathbf{lr}^{(1.1)}$ and $\mathbf{rl}^{(1.2)}$. If $d = 0$ then $\dot{\sigma}_R > 0$ in $\mathbf{lr}^{(1.1)}$, and $\dot{\sigma}_R = 0$ in $\mathbf{rl}^{(1.2)}$. Therefore, the trajectories are convergent to $\mathbf{r}^{(1)}$ from $\mathbf{lr}^{(1.1)}$ and are parallel to $\mathbf{r}^{(1)}$ in $\mathbf{rl}^{(1.2)}$. Otherwise, if $d > 0$ then $\dot{\sigma}_R > 0$, in $\mathbf{lr}^{(1.1)}$, and $\dot{\sigma}_R < 0$, in $\mathbf{rl}^{(1.2)}$. Therefore, we have $\sigma_R \dot{\sigma}_R < 0$, in a neighbourhood of $\mathbf{r}^{(1)}$, and in the closed loop system a sliding motion is enforced on this arc of $\mathbf{r}^{(1)}$, for any disturbance $d(t)$ as in (5).

Region $\mathbf{r}^{(2)}$. Curve $\mathbf{r}^{(2)}$ is on the boundary of $\mathbf{rsr}^{(1)}$ and $\mathbf{rl}^{(1.3)}$. If $d = 0$, since $\dot{\sigma}_R = 0$ in $\mathbf{rsr}^{(1)} \cup \mathbf{rl}^{(1.3)}$ then, the trajectories are parallel to $\mathbf{r}^{(2)}$ in $\mathbf{rsr}^{(1)}$ and $\mathbf{rl}^{(1.3)}$. Otherwise, if $d > 0$, since $\dot{\sigma}_R > 0$ in $\mathbf{rsr}^{(1)} \cup \mathbf{rl}^{(1.3)}$, then, the trajectories across the curve $\mathbf{r}^{(2)}$ from region $\mathbf{rsr}^{(1)}$ to region $\mathbf{rl}^{(1.3)}$.

Region $\mathbf{r}^{(3)}$. Curve $\mathbf{r}^{(3)}$ is a piece of the boundary of $\mathbf{rsr}^{(2)}$ and $\mathbf{lr}^{(2)}$. If $d = 0$ then $\dot{\sigma}_R < 0$, in $\mathbf{lr}^{(2)}$, and $\dot{\sigma}_R = 0$ in $\mathbf{rsr}^{(2)}$. Therefore, the trajectories are convergent to $\mathbf{r}^{(3)}$ from $\mathbf{lr}^{(2)}$ and are parallel to $\mathbf{r}^{(3)}$ in $\mathbf{rsr}^{(2)}$. Otherwise, if $d > 0$, since $\dot{\sigma}_R < 0$ in $\mathbf{rsr}^{(2)} \cup \mathbf{lr}^{(2)}$ then, the trajectories across the curve $\mathbf{r}^{(3)}$ from region $\mathbf{lr}^{(2)}$ to region $\mathbf{rsr}^{(2)}$.

Region $\mathbf{l}^{(1)}$. Curve $\mathbf{l}^{(1)}$ is a piece of the boundary of $\mathbf{lr}^{(1.2)}$ and $\mathbf{rl}^{(1.1)}$. If $d = 0$ then $\dot{\sigma}_L < 0$ in $\mathbf{rl}^{(1.1)}$, and $\dot{\sigma}_L = 0$ in $\mathbf{lr}^{(1.2)}$. Therefore, the trajectories are convergent to $\mathbf{l}^{(1)}$ from $\mathbf{rl}^{(1.1)}$ and are parallel to $\mathbf{l}^{(1)}$ in $\mathbf{lr}^{(1.2)}$. Otherwise, if $d > 0$, since $\dot{\sigma}_L < 0$ in $\mathbf{rl}^{(1.1)} \cup \mathbf{lr}^{(1.2)}$ then, the trajectories across the curve $\mathbf{l}^{(1)}$ from region $\mathbf{rl}^{(1.1)}$ to region $\mathbf{lr}^{(1.2)}$.

Region $\mathbf{l}^{(2)}$. Curve $\mathbf{l}^{(2)}$ is a piece of the boundary of $\mathbf{lr}^{(1.3)}$ and $\mathbf{lsl}^{(1)}$. If $d = 0$, since $\dot{\sigma}_L = 0$ in $\mathbf{lr}^{(1.3)} \cup \mathbf{lsl}^{(1)}$ then, the trajectories are parallel to $\mathbf{l}^{(2)}$ in $\mathbf{lr}^{(1.3)}$ and $\mathbf{lsl}^{(1)}$. Otherwise, if $d > 0$, since $\dot{\sigma}_L > 0$ in $\mathbf{lr}^{(1.3)} \cup \mathbf{lsl}^{(1)}$, then, the trajectories across the curve $\mathbf{l}^{(2)}$ from region $\mathbf{lr}^{(1.3)}$ to region $\mathbf{lsl}^{(1)}$.

Region $\mathbf{l}^{(3)}$. Curve $\mathbf{l}^{(3)}$ is a piece of the boundary of $\mathbf{rl}^{(2)}$ and **lsl**. If $d = 0$ then $\dot{\sigma}_L > 0$ in $\mathbf{rl}^{(2)}$, and $\dot{\sigma}_R = 0$ in $\mathbf{lsl}^{(2)}$. Therefore, the trajectories are convergent to $\mathbf{l}^{(3)}$ from $\mathbf{rl}^{(2)}$ and are parallel to $\mathbf{l}^{(3)}$ in $\mathbf{lsl}^{(2)}$. Otherwise, if $d > 0$, two cases are in order, namely:

- if $d \in (0, \frac{2}{5}]$, trajectories leave $\mathbf{rl}^{(2)}$ to enter $\mathbf{l}^{(3)}$;
- if $d \in (\frac{2}{5}, 1]$, some trajectories
  - may leave $\mathbf{rl}^{(2)}$ to enter $\mathbf{l}^{(3)}$, crossing the boundary at some point with $\tilde{y} \in (1, \frac{d+2}{3d})$;
  - may leave $\mathbf{l}^{(3)}$ to enter $\mathbf{rl}^{(2)}$, crossing the boundary at some point with $\tilde{y} \in (\frac{d+2}{3d}, 2)$.

In the following, we provide upper bounds $L(\cdot)$ for the length of the arc covered by the origin of the Frenet frame along the reference path Γ, when the image of the robot in the reduced state space $(\tilde{y}, \tilde{\theta})$ moves inside a given region of the partion Π reported in Table 1. The expression of the upper bounds $L(\cdot)$ are normalized with respect to the minimum turning radius R. The motion of the origin of the Frenet frame is described by the curvilinear abscissa $s(t)$, whose dynamics is $\dot{s} = \frac{\cos(\tilde{\theta})}{1-\tilde{y}d}\frac{V}{R}$. Hence, given a region $S \in \Pi$, the upper bound $L(S)$ can be obtained by solving, for all possible initial conditions $(\tilde{y}_1, \tilde{\theta}_1) \in S$, an optimal control problem that gives the worst disturbance $d^\star$ for which

$$\int_0^\tau \frac{\cos(\tilde{\theta})}{1-\tilde{y}d}\frac{V}{R}$$

is maximized, subject to the dynamics (14), and up to a time τ such that $(\tilde{y}(\tau), \tilde{\theta}(\tau))$ belongs to the boundary of S.

By solving this optimal control problem we obtain that

- singular solutions correspond to trajectories belonging to either **sr** or **sl**, for which $L(\mathbf{sr}) = L(\mathbf{sl}) = 0$ since the robot tracks a line perpendicular to the reference path Γ.
- for no–singular trajectories, $d^\star$ is constant.

Furthermore, since inside any region S of Π, $\tilde{\theta}(t)$ is monotonic, then the maximum length traveled by the origin of the Frenet frame can be obtained integrating with respect to $\tilde{\theta}$ instead of time. By (14), we have

$$\frac{ds}{d\tilde{\theta}} = \left[\frac{d\tilde{\theta}}{dt}\right]^{-1} \dot{s} = \frac{\Omega\cos(\tilde{\theta})}{1 - \tilde{y}d - \Omega\cos(\tilde{\theta})d}$$

Along trajectories $(\tilde{y}(t), \tilde{\theta}(t))$ obtained with d constant, say $d = D$, the above expression is rewritten as:

$$\frac{ds}{d\tilde{\theta}} = \pm\frac{\Omega\cos(\tilde{\theta})}{\sqrt{P^2 - D^2\sin(\tilde{\theta})^2}} \tag{24}$$

where

$$P^2 = (1 - \tilde{y}_1 D)[1 - \tilde{y}_1 D - 2\Omega\cos(\tilde{\theta}_1)D] + D^2 \tag{25}$$

is a constant parameter and $(\tilde{y}_1, \tilde{\theta}_1)$ is a point which belongs to $(\tilde{y}(t), \tilde{\theta}(t))$. Integrating (24) from $\tilde{\theta}_1$ to $\tilde{\theta}_2$ we obtain

$$s(P, \tilde{\theta}_1, \tilde{\theta}_2) = \begin{cases} \left[\operatorname{asin}\left(\frac{\sin(\tilde{\theta}_2)D}{P}\right) - \operatorname{asin}\left(\frac{\sin(\tilde{\theta}_1)D}{P}\right)\right]\frac{\Omega}{D} \\ \qquad\qquad \text{if } D \neq 0 \\ \left[\sin(\tilde{\theta}_2) - \sin(\tilde{\theta}_1)\right]\Omega \\ \qquad\qquad \text{if } D = 0 \end{cases} \tag{26}$$

In any interval $[k\frac{\pi}{2}, (k+1)\frac{\pi}{2}]$, $s(P, \tilde{\theta}_1, \tilde{\theta}_2)$ as in (26), is monotonic with respect to both $\tilde{\theta}_1$ and $\tilde{\theta}_2$. Hence, the maximum of $s(P, \tilde{\theta}_1, \tilde{\theta}_2)$ is achieved for $\tilde{\theta}_1$ and $\tilde{\theta}_2$ on the extreme points $k\frac{\pi}{2}$ and $(k+1)\frac{\pi}{2}$. So, maximizing (26), we get

$$s(P) = \max_{\tilde{\theta}_1, \tilde{\theta}_2} s(P, \tilde{\theta}_1, \tilde{\theta}_2) = \begin{cases} \frac{1}{D}\operatorname{asin}\left(\frac{D}{P}\right) & \text{if } D \neq 0 \\ 1 & \text{if } D = 0 \end{cases} \tag{27}$$

where, by (25), P can be expressed in terms of points $\tilde{\theta}_i = k\pi$ (with i either 1 or 2) as follows

$$P = \begin{cases} 1 - (\tilde{y} + \Omega)D & \text{if } \tilde{\theta} = 0 \\ 1 - (\tilde{y} - \Omega)D & \text{if } \tilde{\theta} \in \{-\pi, +\pi\} \end{cases} \tag{28}$$

Regions $\mathbf{rsr}^{(1)}$, $\mathbf{rsr}^{(2)}$, $\mathbf{lsr}^{(1)}$ and $\mathbf{lsr}^{(2)}$. By (14) and (28), $P = 1 - (\tilde{y} + 1)D$. For $\tilde{y} \leq -1$, $\tilde{y} + 1 \leq 0$ and, since $D \geq 0$, then $P \geq 1$. Hence, $\frac{1}{D}\operatorname{asin}\left(\frac{D}{P}\right) \leq \frac{1}{D}\operatorname{asin}(D) \leq \frac{\pi}{2}$. Then, the maximum length of the arc traveled by the origin of the Frenet frame along the reference path Γ is obtained with $d = 1$, i.e. $L(\mathbf{rsr}^{(1)}) = L(\mathbf{rsr}^{(2)}) = L(\mathbf{lsr}^{(1)}) = L(\mathbf{lsr}^{(2)}) = \frac{\pi}{2}$.

Regions $\mathbf{lr}^{(1.1)}$, $\mathbf{lr}^{(1.2)}$ and $\mathbf{rl}^{(1.3)}$. By (14) and (28), $P = 1 - (\tilde{y} + 1)D$. According to the case $\mathbf{lsr}^{(1)}$, when $\tilde{y} \leq -1$ an upper bound for $s(P)$ is $\frac{\pi}{2}$. However, when $-1 < \tilde{y} \leq 1$, since the excursion of $\tilde{\theta}$ is lower than $\frac{\pi}{2}$, then path traveled by the origin is smaller. Hence, $L(\mathbf{lr}^{(1.1)}) = L(\mathbf{lr}^{(1.2)}) = L(\mathbf{rl}^{(1.3)}) = \frac{\pi}{2}$.

Regions $\mathbf{rl}^{(1.1)}$, $\mathbf{rl}^{(1.2)}$ and $\mathbf{lr}^{(1.3)}$. By (14) and (28), $P = 1 + (1 - \tilde{y})D$. Remind that, by (11), $\tilde{y}D < 1$. Hence, choosing D arbitrarily close to $\tilde{y}^{-1}$, $\frac{D}{P} = \frac{D}{D + (1 - \tilde{y}D)}$ goes arbitrarily close to 1. Then $s(P)$ is upper bounded by $\frac{\pi}{2}\frac{1}{D} < \frac{\pi}{2}\tilde{y}$. Further, $\tilde{y}$ is upper bounded by both 2 (by definition of $\mathbf{rl}^{(1.1)}$, $\mathbf{rl}^{(1.2)}$ and $\mathbf{lr}^{(1.3)}$) and C^{-1}. Hence, $L(\mathbf{rl}^{(1.1)}) = L(\mathbf{rl}^{(1.2)}) = L(\mathbf{lr}^{(1.3)}) = \frac{\pi}{2}\min(2, C^{-1})$.

Regions $\mathbf{rsl}^{(1)}$, $\mathbf{rsl}^{(2)}$, $\mathbf{lsl}^{(1)}$ and $\mathbf{lsl}^{(2)}$. Recall that the trajectory is bounded to belong to $\mathcal{I}_{(\tilde{y},\tilde{\theta})}(C)$. Then, similarly to the above, $\frac{D}{P} = \frac{D}{D+(1-\tilde{y}D)}$ may go arbitrarily close to 1, by choosing D arbitrarily close to $\tilde{y}^{-1}$. Hence, $s(P)$ is upper bounded by $\frac{\pi}{2}\frac{1}{D} < \frac{\pi}{2}\tilde{y} \leq \frac{\pi}{2}C^{-1}$, and $L(\mathbf{rsl}^{(1)}) = L(\mathbf{rsl}^{(2)}) = L(\mathbf{lsl}^{(1)}) = L(\mathbf{lsl}^{(2)}) = \frac{\pi}{2}C^{-1}$.

Regions $\mathbf{r}^{(1)}$ and $\mathbf{lr}^{(2)}$. In the closed loop system, a sliding motion takes place along the arc $\mathbf{r}^{(1)}$. By (14) and (28) $P = 1 - \tilde{y}D + D$. For $\tilde{y} \leq 0$ and $D \geq 0$, then $P \geq 1$. Hence, $\frac{1}{D}\text{asin}\left(\frac{D}{P}\right) \leq \frac{1}{D}\text{asin}(D) \leq \frac{\pi}{2}$, and $L(\mathbf{r}^{(1)}) = \frac{\pi}{2}$. Since, the same bounds hold for region $\mathbf{lr}^{(2)}$, we obtain $L(\mathbf{lr}^{(2)}) = \frac{\pi}{2}$, as well.

Regions $\mathbf{r}^{(2)}$, $\mathbf{r}^{(3)}$, $\mathbf{l}^{(1)}$ and $\mathbf{l}^{(2)}$. The robot moves along this boundaries only if $d = 0$. Hence, the upper bounds are $L(\mathbf{r}^{(2)}) = L(\mathbf{r}^{(3)}) = L(\mathbf{l}^{(1)}) = L(\mathbf{l}^{(2)}) = 1$.

Region $\mathbf{l}^{(3)}$. In the closed loop system, a sliding motion takes place along the arc $\mathbf{l}^{(3)}$ for $\tilde{y} \in (0, \frac{1+2d}{3})$, or when $d = 0$ (the latter would give bound 1). The longest piece of sliding motion is obtained with $d = 1$. By (14) and (28), $P = 1 - \tilde{y}D + D \geq 1$. Hence, $\frac{1}{D}\text{asin}\left(\frac{D}{P}\right) \leq \frac{1}{D}\text{asin}(D) \leq \frac{\pi}{2}$, and $L(\mathbf{l}^{(3)}) = \frac{\pi}{2}$.

Regions $\mathbf{rl}^{(2)}$. An upper bound for $L(\mathbf{rl}^{(2)})$ can be more easily obtained in the robot motion space. See Figure 7. When $D > \frac{1}{2}$, under control $\Omega = -1$ from an initial configuration P_1 with lateral error $\tilde{y} = \epsilon$ and orientation error $\tilde{\theta} = -\pi^+$, with $\epsilon > 0$ small enough, the robot performs a rotation of π radiant, around the center of the reference circle, and reaches the configuration P_2 (assuming no control switch occurs meanwhile), with lateral error $\tilde{y} = \frac{2}{D} - (2+\epsilon)$ and orientation error $\tilde{\theta} = -\pi^+$. Then, it leaves the region $\mathbf{rl}^{(2)}$ to enter region $\mathbf{rl}^{(1.3)}$. Hence, the space traveled by the car along the reference path is over bounded by $L(\mathbf{rl}^{(2)}) = \pi$.

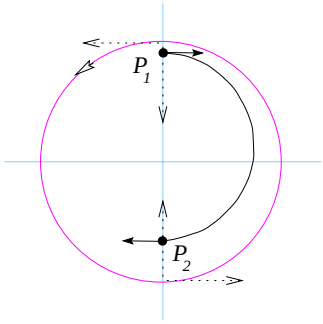

Figure 7: Worst path in region $\mathbf{rl}^{(2)}$.

The upper bounds for the space traveled by the origin of the Frenet frame in each region are summarized in Table 2. The proof of Proposition 2 is completed by associating to all outgoing arc of each node of the graph

regions	$L()$
sr, **sl**	0
$\mathbf{rsr}^{(1)}$, $\mathbf{rsr}^{(2)}$, $\mathbf{lsr}^{(1)}$, $\mathbf{lsr}^{(2)}$, $\mathbf{lr}^{(1.1)}$, $\mathbf{lr}^{(1.2)}$, $\mathbf{rl}^{(1.3)}$, $\mathbf{lr}^{(2)}$ $\mathbf{r}^{(1)}$, $\mathbf{l}^{(3)}$	$\frac{\pi}{2}$
$\mathbf{rl}^{(1.1)}$, $\mathbf{rl}^{(1.2)}$, $\mathbf{lr}^{(1.3)}$	$\frac{\pi}{2}\min(2, C^{-1})$
$\mathbf{rsl}^{(1)}$, $\mathbf{rsl}^{(2)}$, $\mathbf{lsl}^{(1)}$, $\mathbf{lsl}^{(2)}$	$\frac{\pi}{2}C^{-1}$
$\mathbf{r}^{(2)}$, $\mathbf{r}^{(3)}$, $\mathbf{l}^{(1)}$, $\mathbf{l}^{(2)}$	1
$\mathbf{rl}^{(2)}$	π

Table 2: Upper bounds for the length of the corresponding arc of the reference path Γ spanned by the origin of the Frenet frame.

FSM_{PTC} , reported in Figure 8, a weight corresponding to the upper bounds obtained in Table 2.

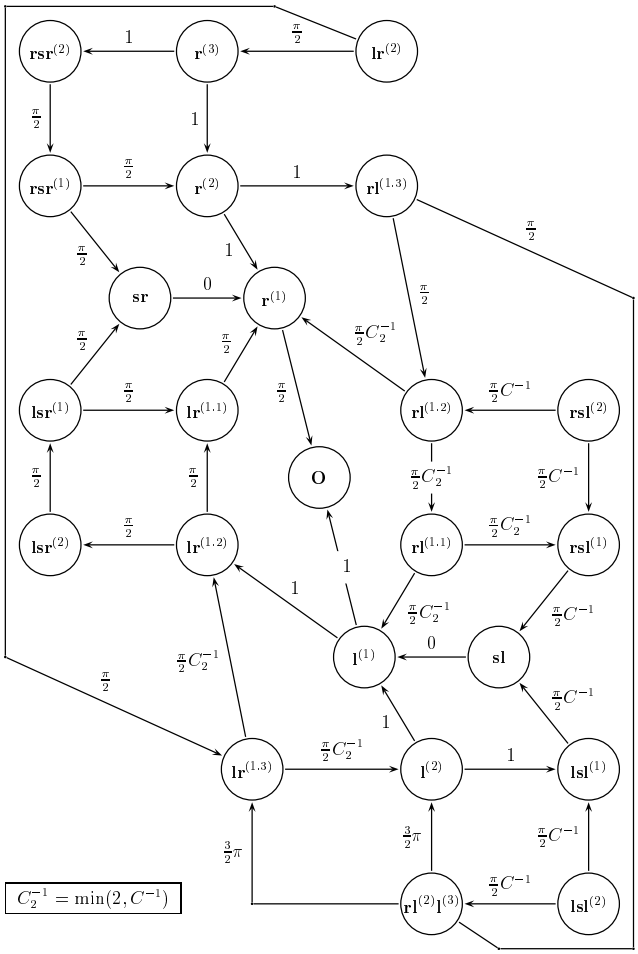

Figure 8: Quotient system FSM_{PTC} representing the behaviour of the closed–loop hybrid system *CLHA* , when $\sigma_r = \epsilon$.

If the reference path Γ has curvature always of the same sign, the convergence of Dubins' car to the path is guaranteed by:

Corollary 1 *If the reference path* Γ *has curvature always of the same sign and amplitude lower than* $\frac{1}{2R}$*, the hybrid feedback control (7) and (9), ensures the tracking of* Γ *for any initial vehicle configuration in the domain* $\mathcal{I}_{(\tilde{y},\tilde{\theta})}$ *as in (13). The origin of the Frenet's frame covers at most a distance of*

$$\begin{cases} 1 + \frac{9}{2}\pi + \frac{\pi}{C} & \text{if } C \in [0, \frac{\pi}{6+5\pi}) \\ 4 + 7\pi + \frac{\pi}{2C} & \text{if } C \in [\frac{\pi}{6+5\pi}, \frac{1}{2}) \end{cases} \tag{29}$$

along the reference path Γ *before the vehicle approaches it with correct orientation.*

The proof of the above corollary is obtained by computing the longest path to the node **O**.

By Proposition 2, if Γ is a straight line then the closed–loop system enforces *sliding* motions (see [15] for a tutorial) in the space $(\tilde{y}, \tilde{\theta})$ on the lines **sr**, **sl** and the arcs $\mathbf{r}^{(1)}$, $\mathbf{l}^{(1)}$, $\mathbf{r}^{(3)}$, $\mathbf{l}^{(3)}$ until the origin is reached. If the reference path Γ is not a straight line, sliding motions are enforced only on the lines **sr**, **sl**, on the arcs $\mathbf{r}^{(1)}$, $\mathbf{r}^{(3)}$ and on a piece of the arc $\mathbf{l}^{(3)}$. Under ideal sliding motion, around the origin the control ω switches at infinite frequency between $\frac{V}{R}, 0$ and $-\frac{V}{R}$. The mean value of such control (i.e. the *equivalent control*) is the signal κV that makes the car follow the reference path Γ with velocity V. In the real implementation smoothing techniques are applied to avoid the chattering of the control signal between the three values $\frac{V}{R}, 0$ and $-\frac{V}{R}$.

The behaviour of the closed–loop system *CLHA* under the action of the discrete disturbance σ_r is characterized by the following propositions.

Proposition 3 *Given an initial condition $(\tilde{y}_0, \tilde{\theta}_0)$ in the open neighbourhood of the origin*

$$\mathcal{N}_{(\tilde{y},\tilde{\theta})} = \left\{ (\tilde{y},\tilde{\theta}) : |\tilde{y}| < 1, -\arccos\left(\frac{1}{2} - \frac{\tilde{y}}{2}\right) < \tilde{\theta} < \arccos\left(\frac{1}{2} + \frac{\tilde{y}}{2}\right) \right\} \tag{30}$$

(see Figure 9), the hybrid closed–loop system CLHA keeps the continuous–time trajectory $(\tilde{y}(t), \tilde{\theta}(t))$ inside $\mathcal{N}_{(\tilde{y},\tilde{\theta})}$, under any disturbance $d(t)$ bounded as in (5) and any sequence of events σ_r.

Proof of Proposition 3. In the sequel, applying a reachability analysis, we show that the hybrid system *CLHA* under the action of the continuous disturbance $d(t)$ and the discrete disturbance σ_r keeps the trajectories inside $\mathcal{N}_{(\tilde{y},\tilde{\theta})}$.

First of all, notice that $\mathcal{N}_{(\tilde{y},\tilde{\theta})}$ is symmetric with respect to the origin. Therefore, states in $\mathcal{N}_{(\tilde{y},\tilde{\theta})}$ remain inside $\mathcal{N}_{(\tilde{y},\tilde{\theta})}$ after any state reset $\tilde{y} := -\tilde{y}$ and $\tilde{\theta} := -\tilde{\theta}$ due to an event $\sigma_r = \textit{switch}$.

Consider a partition of the set $\mathcal{N}_{(\tilde{y},\tilde{\theta})}$ into the sets $\mathbf{r}^{(1)} \backslash \{(-1, \frac{\pi}{2})\}$, $\mathbf{l}^{(1)} \backslash \{(1, -\frac{\pi}{2})\}$, $\mathbf{lr}^{(1.1)} \cap \mathcal{N}_{(\tilde{y},\tilde{\theta})}$, $\mathbf{rl}^{(1.1)} \cap \mathcal{N}_{(\tilde{y},\tilde{\theta})}$, $\mathbf{rl}^{(1)} \cap \mathcal{N}_{(\tilde{y},\tilde{\theta})}$, and $\mathbf{lr}^{(1.2)} \cap \mathcal{N}_{(\tilde{y},\tilde{\theta})}$.

Region $\mathbf{r}^{(1)} \backslash \{(-1, \frac{\pi}{2})\}$. According to Proposition 2, the state $(\tilde{y}, \tilde{\theta})$ is steered to the origin with $\|(\tilde{y}(t), \tilde{\theta}(t))\|$ monotonicly decreasing. Under the action of an event $\sigma_r = \textit{switch}$, the state jumps instantaneously to the symmetric point in $\mathbf{l}^{(1)} \setminus \{(1, -\frac{\pi}{2})\}$.

Region $\mathbf{l}^{(1)} \setminus \{(1, -\frac{\pi}{2})\}$. According to Proposition 2, either the state $(\tilde{y}, \tilde{\theta})$ is steered to the origin if $d(t) = \infty$ ($\|(\tilde{y}(t), \tilde{\theta}(t))\|$ monotonicly decreasing) or enters region $\mathbf{lr}^{(1.2)}$ if $d(t) < \infty$ at some $\tilde{\theta} > -\frac{\pi}{2}$. Under the action of an event $\sigma_r = \textit{switch}$, the state jumps instantaneously to the symmetric point in $\mathbf{r}^{(1)} \setminus \{(-1, \frac{\pi}{2})\}$.

Region $\mathbf{lr}^{(1.1)} \cap \mathcal{N}_{(\tilde{y},\tilde{\theta})}$. The hybrid system *CLHA* is in mode $\textit{mode} = \textit{positive}$. By (1), $\tilde{y} < 0$ and Therefore, by (5), we have $0 < \frac{1}{d(t)-\tilde{y}} < 1$. From (14), $\dot{\tilde{\theta}} > 0$ and $\dot{\tilde{y}} > 0$. Then, any state $(\tilde{y}, \tilde{\theta}) \in \mathbf{lr}^{(1.1)} \cap \mathcal{N}_{(\tilde{y},\tilde{\theta})}$ is steered to $\mathbf{r}^{(1)} \setminus \{(-1, \frac{\pi}{2})\}$. If an event $\sigma_r = \textit{switch}$ occurs, the state jumps instantaneously to the symmetric point in region $\mathbf{rl}^{(1.1)} \cap \mathcal{N}_{(\tilde{y},\tilde{\theta})}$.

Region $\mathbf{rl}^{(1.1)} \cap \mathcal{N}_{(\tilde{y},\tilde{\theta})}$. The hybrid system *CLHA* is in mode $\textit{mode} = \textit{negative}$. By (14), $\dot{\tilde{\theta}} < 0$ and $\dot{\tilde{y}} < 0$. Then, any state $(\tilde{y}, \tilde{\theta}) \in \mathbf{lr}^{(1.1)} \cap \mathcal{N}_{(\tilde{y},\tilde{\theta})}$ is steered to $\mathbf{l}^{(1)} \setminus \{(1, -\frac{\pi}{2})\}$. If an event $\sigma_r = \textit{switch}$ occurs the state jumps instantaneously to the symmetric point in region $\mathbf{lr}^{(1.1)} \cap \mathcal{N}_{(\tilde{y},\tilde{\theta})}$.

Region $\mathbf{rl}^{(1.2)} \cap \mathcal{N}_{(\tilde{y},\tilde{\theta})}$. The hybrid system *CLHA* is in mode $\textit{mode} = \textit{negative}$. Consider the function $\sigma_{\mathcal{N}}^{up}(\tilde{y}, \tilde{\theta}) = -1 - \tilde{y} + 2\cos(\tilde{\theta})$ and observe that, within region $\mathbf{rl}^{(1.2)}$, $\sigma_{\mathcal{N}}^{up}(\tilde{y}, \tilde{\theta}) > 0 \Leftrightarrow (\tilde{y}, \tilde{\theta}) \in \mathcal{N}_{(\tilde{y},\tilde{\theta})}$. By (14) $\dot{\sigma}_{\mathcal{N}}^{up} = \sin(\tilde{\theta}) \left(1 + 2\frac{\cos(\tilde{\theta})}{d(t)-\tilde{y}}\right) \frac{U}{R} > 0$ for all states within this region, except for $\tilde{\theta} = 0$. Therefore, any trajectory originating in $\mathbf{rl}^{(1.2)} \cap \mathcal{N}_{(\tilde{y},\tilde{\theta})}$ cannot escape the region through the upper boundary $\sigma_{\mathcal{N}}^{up} = 0$, and will either reach the sliding surface $\mathbf{r}^{(1)} \setminus \{(-1, \frac{\pi}{2})\}$ (for some $\tilde{\theta} > 0$), pass to $\mathbf{rl}^{(1.1)} \cap \mathcal{N}_{(\tilde{y},\tilde{\theta})}$ through the boundary $\tilde{\theta} = 0$, or jump symmetrically to $\mathbf{lr}^{(1.2)} \cap \mathcal{N}_{(\tilde{y},\tilde{\theta})}$ under the action of an event $\sigma_r = \textit{switch}$.

Region $\mathbf{lr}^{(1.2)} \cap \mathcal{N}_{(\tilde{y},\tilde{\theta})}$. The hybrid system *CLHA* is in mode $\textit{mode} = \textit{positive}$. Consider the function $\sigma_{\mathcal{N}}^{dw}(\tilde{y}, \tilde{\theta}) = -1 + \tilde{y} + 2\cos(\tilde{\theta})$. Within this region, we have $\sigma_{\mathcal{N}}^{dw}(\tilde{y}, \tilde{\theta}) < 1$ and $\sigma_{\mathcal{N}}^{dw}(\tilde{y}, \tilde{\theta}) > 0 \Leftrightarrow (\tilde{y}, \tilde{\theta}) \in \mathcal{N}_{(\tilde{y},\tilde{\theta})}$. Further, by (14), $\dot{\sigma}_{\mathcal{N}}^{dw} = -\sin(\tilde{\theta}) \left(1 - 2\frac{\cos(\tilde{\theta})}{d(t)-\tilde{y}}\right) \frac{U}{R}$. Therefore, for any $\tilde{\theta} \neq 0$, $\dot{\sigma}_{\mathcal{N}}^{dw}(\tilde{y}, \tilde{\theta}) > 0 \;\Leftrightarrow\; 0 < \sigma_{\mathcal{N}}^{dw}(\tilde{y}, \tilde{\theta}) < d(t) - 1$. Since $\sigma_{\mathcal{N}}^{dw}(\tilde{y}, \tilde{\theta})$ always increases except for $\sigma_{\mathcal{N}}^{dw}(\tilde{y}, \tilde{\theta}) > d(t) - 1$, being by (5) $d(t) - 1$ nonnegative, $(\tilde{y}, \tilde{\theta})$ never crosses the boundary $\sigma_{\mathcal{N}}^{dw}(\tilde{y}, \tilde{\theta}) = 0$. Then, trajectories originating in $\mathbf{lr}^{(1.2)} \cap \mathcal{N}_{(\tilde{y},\tilde{\theta})}$ cannot leave this region through the boundary $\sigma_{\mathcal{N}}^{dw} = 0$. Instead, they may leave region $\mathbf{lr}^{(1.2)} \cap \mathcal{N}_{(\tilde{y},\tilde{\theta})}$ either through the boundary with $\mathbf{lr}^{(1.1)} \cap \mathcal{N}_{(\tilde{y},\tilde{\theta})}$, $\tilde{\theta} = 0$, with $\tilde{y} > -1$, or by jumping symmetrically to region $\mathbf{rl}^{(1.2)} \cap \mathcal{N}_{(\tilde{y},\tilde{\theta})}$ for an event $\sigma_r = \textit{switch}$.

Proposition 4 *If the reference path Γ is such that changes in the curvature sign are at distance greater than $(5 + \frac{\pi}{2})R$ along it, then the hybrid feedback control (7), with modes chosen according to (9) stabilizes Dubins' car along the reference path Γ.*

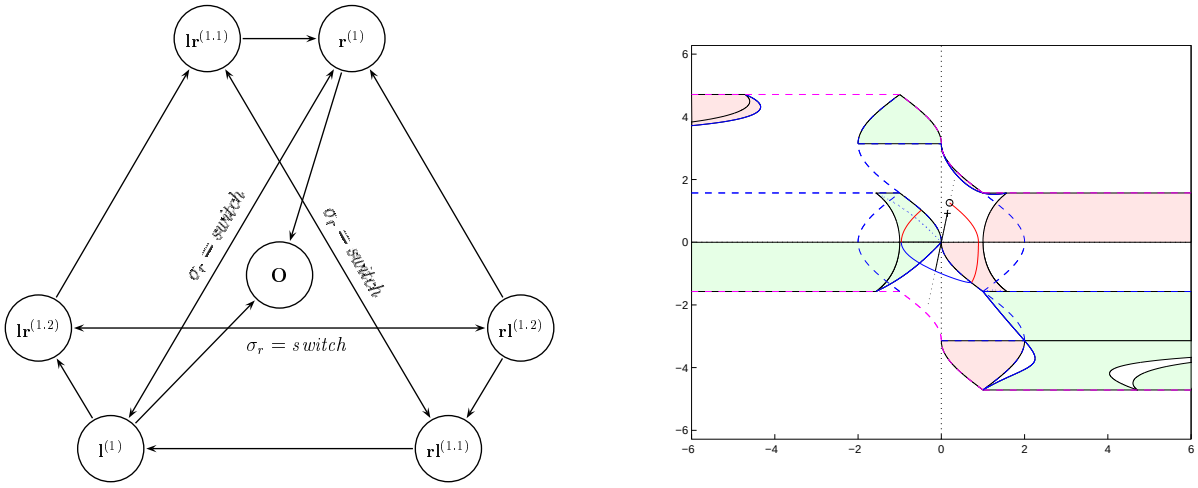

Figure 9: On the left:quotient system FSM^{D}_{PTC} representing the behaviour of the closed–loop hybrid system *CLHA* , when the initial state belongs to $\mathcal{O}\times\mathcal{N}_{(\tilde{y},\tilde{\theta})}$. On the right: regions in the domain $\mathcal{D}_{(\tilde{y},\tilde{\theta})}$ where $\dot{W}>0$.

T. he set $\mathcal{N}_{(\tilde{y},\tilde{\theta})}$ defined in (30) is such that

$$\mathcal{N}_{(\tilde{y},\tilde{\theta})} \subset \mathbf{O}\cup\mathbf{r}^{(1)}\cup\mathbf{l}^{(1)}\cup\mathbf{lr}^{(1.1)}\cup\mathbf{lr}^{(1.2)}\cup\mathbf{rl}^{(1.1)}\cup\mathbf{rl}^{(1.2)}\ .$$

Since, by Proposition 3, $\mathcal{N}_{(\tilde{y},\tilde{\theta})}$ is a robust invariant set for the closed–loop hybrid system *CLHA* , then, if we restrict our attention to the domain $\mathcal{N}_{(\tilde{y},\tilde{\theta})}$, the transitions from $\mathbf{lr}^{(1.2)}$ to $\mathbf{lsr}^{(2)}$ and from $\mathbf{rl}^{(1.1)}$ to $\mathbf{rsl}^{(1)}$ in the quotient system FSM_{PTC} should be removed. Furthermore, notice that, under the action of the discrete disturbance $\sigma_r = switch$, the reset $\tilde{y} := -\tilde{y}$ and $\tilde{\theta} := -\tilde{\theta}$ introduces the mutual transitions $\mathbf{r}^{(1)} \leftrightarrows \mathbf{l}^{(1)}$, $\mathbf{lr}^{(1.1)} \leftrightarrows \mathbf{rl}^{(1.1)}$, and $\mathbf{lr}^{(1.2)} \leftrightarrows \mathbf{rl}^{(1.2)}$. Hence, in the presence of the discrete disturbance σ_r and for any disturbance d as in (5), when the initial state belongs to $\mathcal{O}\times\mathcal{N}_{(\tilde{y},\tilde{\theta})}$, the quotient system FSM^{D}_{PTC} obtained from the equivalent relation $\sim$ is as in Figure 9.

To analyze the convergence of the trajectories to $\mathbf{O}$, introduce the function

$$W(\tilde{y},\tilde{\theta}) = \frac{1}{2}(\tilde{y}^2+\tilde{\theta}^2). \tag{31}$$

$W(\tilde{y},\tilde{\theta})$ has the property that, if at time $t=\bar{t}$, $\sigma_r = switch$, then $W(\tilde{y}(\bar{t}),\tilde{\theta}(\bar{t})) = W(\tilde{y}(\bar{t}^-),\tilde{\theta}(\bar{t}^-))$. The derivative with respect to time of W evaluates to

$$\dot{W}(\tilde{y},\tilde{\theta}) = \left[\tilde{y}\sin(\tilde{\theta}) - \tilde{\theta}\frac{\cos(\tilde{\theta})d}{1-\tilde{y}d} - \tilde{\theta}\varpi\right]\frac{V}{R}, \tag{32}$$

where $\varpi = 0,-1$, and 1 in mode *zero*, *negative*, and *positive*, respectively. The study of the sign of $\dot{W}(\tilde{y},\tilde{\theta})$ is extended to the entire domain $\mathcal{D}_{(\tilde{y},\tilde{\theta})}$. Under assumption (11), multiplying (32) by $\frac{R}{V}(1-\tilde{y}d)$, we have

$$\dot{W}>0 \ \Leftrightarrow\ \mu(\tilde{y},\tilde{\theta}) = d\left[-\tilde{y}^2\sin(\tilde{\theta}) - \tilde{\theta}\cos(\tilde{\theta}) + \varpi\tilde{y}\tilde{\theta}\right] + \left[\tilde{y}\sin(\tilde{\theta}) - \varpi\tilde{\theta}\right] > 0,$$

for some disturbance d bounded as in (5). Hence, for any $(\tilde{y},\tilde{\theta})$ such that $\eta_1(\tilde{y},\tilde{\theta}) = \tilde{y}\sin(\tilde{\theta}) - \varpi\tilde{\theta} > 0$, there exists d as in (5) such that $\mu(\tilde{y},\tilde{\theta})>0$ and $\dot{W}>0$. Otherwise, if $(\tilde{y},\tilde{\theta})$ is such that $\eta_1(\tilde{y},\tilde{\theta})<0$, then there exists d as in (5) such that $\dot{W}>0$ if and only if $\mu(\tilde{y},\tilde{\theta})$ is positive for $d=1$. That is, if

$$\eta_2(\tilde{y},\tilde{\theta}) = -\sin(\tilde{\theta})\tilde{y}^2 + \left[\sin(\tilde{\theta}) + \varpi\tilde{\theta}\right]\tilde{y} - \left[\tilde{\theta}\cos(\tilde{\theta}) + \varpi\tilde{\theta}\right] > 0.$$

The regions in the domain $\mathcal{D}_{(\tilde{y},\tilde{\theta})}$ where function (31) locally increases are reported in Figure 9. Such regions are delimited by the curves $\eta_1(\tilde{y},\tilde{\theta})=0$ and $\eta_2(\tilde{y},\tilde{\theta})=0$. By (32), the continuous disturbance d that maximizes $\dot{W}(t)$ is

$$d^\star = \begin{cases} 1 & \text{if } \tilde{\theta}\cos(\tilde{\theta})<0 \qquad \text{i.e. } \tilde{\theta}\in(-\frac{\pi}{2},0)\cup(\frac{\pi}{2},\frac{3}{2}\pi) \\ 0 & \text{if } \tilde{\theta}\cos(\tilde{\theta})>0 \qquad \text{i.e. } \tilde{\theta}\in(-\frac{3}{2}\pi,-\frac{\pi}{2})\cup(0,\frac{\pi}{2}) \end{cases} . \tag{33}$$

Consider an initial condition $(\tilde{y}_0,\tilde{\theta}_0)$ in a neighbourhood of the origin contained in $\mathcal{N}_{(\tilde{y},\tilde{\theta})}\cap \mathbf{rl}^{(1.2)}$. At the initial time, the hybrid model *CLHA* is in mode *negative*. Let us assume that $\sigma_r=\epsilon$, for the moment, and let us analyze the evolution of the hybrid model *CLHA* (see Figure 9). Under the action of the worst disturbance (33), the trajectory $(\tilde{y}(t),\tilde{\theta}(t))$ originating from $(\tilde{y}_0,\tilde{\theta}_0)$ reaches the curves $\mathbf{r}^{(1)}$. First $W(t)$ decreases (in $\mathbf{rl}^{(1.2)}$), then it increases (in $\mathbf{rl}^{(1.1)}$). Hence, *mode* switches to *positive*. $W(t)$ decreases (in the first part of $\mathbf{lr}^{(1.2)}$), and it increases again later on (in $\mathbf{lr}^{(1.2)}$ and $\mathbf{lr}^{(1.1)}$) until $(\tilde{y}(t),\tilde{\theta}(t))$ reaches $\mathbf{r}^{(1)}$. Finally, following a sliding motion along the curve $\mathbf{r}^{(1)}$, $(\tilde{y}(t),\tilde{\theta}(t))$ reaches the origin.

Along this trajectory $W(t)$ assumes two local maxima, which correspond to the intersections of $\mathbf{l}^{(1)}$ and $\mathbf{r}^{(1)}$, and two local minima: the first on the line $\tilde{\theta}=0$ when $\tilde{y}>0$, and the second inside region $\mathbf{rl}^{(1.2)}$. Let $\delta=\|(\tilde{y}_0,\tilde{\theta}_0)\|$. Since the trajectory $(\tilde{y}(t),\tilde{\theta}(t))$ is continuous with respect to the initial condition $(\tilde{y}_0,\tilde{\theta}_0)$, then there exist two continuous functions $\zeta_{\max},\zeta_{\min}:\mathbb{R}\to\mathbb{R}$ such that

$$\max_d \max_t \|(\tilde{y}(t),\tilde{\theta}(t))\| = \zeta_{\max}(\delta), \quad \min_d \min_t \|(\tilde{y}(t),\tilde{\theta}(t))\| = \zeta_{\min}(\delta). \tag{34}$$

Further, since the local maximum and minimum points tend to the origin as $\|(\tilde{y}_0,\tilde{\theta}_0)\|$ tends to zero, then $\lim_{\delta\to 0}\zeta_{\max}(\delta)=0$ and $\lim_{\delta\to 0}\zeta_{\min}(\delta)=0$.

Suppose now that a discrete disturbance $\sigma_r=$ *switch* occurs at the precise time $\bar{t}$ at which $(\tilde{y}(\bar{t}^-),\tilde{\theta}(\bar{t}^-))$ is opposite to $(\tilde{y}_0,\tilde{\theta}_0)$ with respect to the origin. Then, the state $(\tilde{y}(\bar{t}^-),\tilde{\theta}(\bar{t}^-))$ is reset to $(\tilde{y}(\bar{t}),\tilde{\theta}(\bar{t}))=(-\tilde{y}(\bar{t}^-),-\tilde{\theta}(\bar{t}^-))\in\mathcal{N}_{(\tilde{y},\tilde{\theta})}$, which lies on the same line to the origin of $(\tilde{y}_0,\tilde{\theta}_0)$. If $W(\tilde{y}_0,\tilde{\theta}_0)>W(\tilde{y}(\bar{t}),\tilde{\theta}(\bar{t}))=W(-\tilde{y}(\bar{t}^-),-\tilde{\theta}(\bar{t}^-))$ then the convergence is preserved. But, if $W(\tilde{y}_0,\tilde{\theta}_0)<W(\tilde{y}(\bar{t}),\tilde{\theta}(\bar{t}))=W(-\tilde{y}(\bar{t}^-),-\tilde{\theta}(\bar{t}^-))$ then, under the action of the discrete disturbance $\sigma_r=$ *switch*, the state $(\tilde{y},\tilde{\theta})$ is reset to a point farther away from the origin than the initial state $(\tilde{y}_0,\tilde{\theta}_0)$ and convergence can be lost.

However, if the reference path Γ is such that changes in the curvature sign are at a distance greater than $(5+\frac{\pi}{2})R$ along it, between to successive actions of the discrete disturbance σ_r, the state $(\tilde{y},\tilde{\theta})$ has enough time to reach the origin. In fact, assuming that, in the worst case, $(\tilde{y}(\bar{t}),\tilde{\theta}(\bar{t}))\in\mathcal{N}_{(\tilde{y},\tilde{\theta})}\cap\mathbf{rl}^{(1.2)}$, an upper bound on the length the arc of Γ spanned by the origin of the Frenet's frame as $(\tilde{y}(t),\tilde{\theta}(t))$ converges to the origin, is given by $L(\mathbf{rl}^{(1.2)})+L(\mathbf{rl}^{(1.1)})+L(\mathbf{l}^{(1)})+L(\mathbf{lr}^{(1.2)})+L(\mathbf{lr}^{(1.1)})+L(\mathbf{r}^{(1)})$ that, according to the weights reported on the quotient system FSM_{PTC} depicted in Figure 8, evaluates to $(5+\frac{\pi}{2})R$.

To prove the robust stabilization of the car along the reference path Γ we have to show that for any $\epsilon>0$, there exists $\delta>0$ such that any trajectory $(\tilde{y}(t),\tilde{\theta}(t))$ of the hybrid system *CLHA* , originating from any $(\tilde{y}_0,\tilde{\theta}_0)$ with $\|(\tilde{y}_0,\tilde{\theta}_0)\|<\delta$, we have $\|(\tilde{y}(t),\tilde{\theta}(t))\|<\epsilon$. Given any $\epsilon>0$, consider any initial condition $(\tilde{y}_0,\tilde{\theta}_0)$ with

$$\|(\tilde{y}_0,\tilde{\theta}_0)\|\le\delta=\zeta_{\max}^{-1}(\zeta_{\min}^{-1}(\zeta_{\max}^{-1}(\epsilon))). \tag{35}$$

The trajectory $(\tilde{y}(t),\tilde{\theta}(t))$ evolves inside a ball of radius $\zeta_{\min}^{-1}(\zeta_{\max}^{-1}(\epsilon))$. If a disturbance $\sigma_r=$ *switch* occurs at some time $\bar{t}$, then the state is reset to $(\tilde{y}(\bar{t}),\tilde{\theta}(\bar{t}))=(-\tilde{y}(\bar{t}^-),-\tilde{\theta}(\bar{t}^-))\in\mathcal{N}_{(\tilde{y},\tilde{\theta})}$. In the evolution for $t>\bar{t}$ the trajectory reaches the origin before a further discrete disturbance occurs. Moreover, since $\|(\tilde{y}(\bar{t}),\tilde{\theta}(\bar{t})\|\le\zeta_{\min}^{-1}(\zeta_{\max}^{-1}(\epsilon))$ then, the trajectory $(\tilde{y}(t),\tilde{\theta}(t))$ for $t>\bar{t}$ does not exit a ball of radius $\zeta_{\max}(\zeta_{\max}^{-1}(\epsilon))=\epsilon$. Then, the hybrid feedback control (7), with modes chosen according to (9) robustly stabilizes the car along the reference path Γ.

5 Experimental Results

Experiments were devised to assess practicality of the proposed methods against discrepancies of our models from real-world implementation, such as nonnegligible dynamics, disturbances in state measurements, and low sampling and communication time. The system used for experiments is the same of that described in [13],

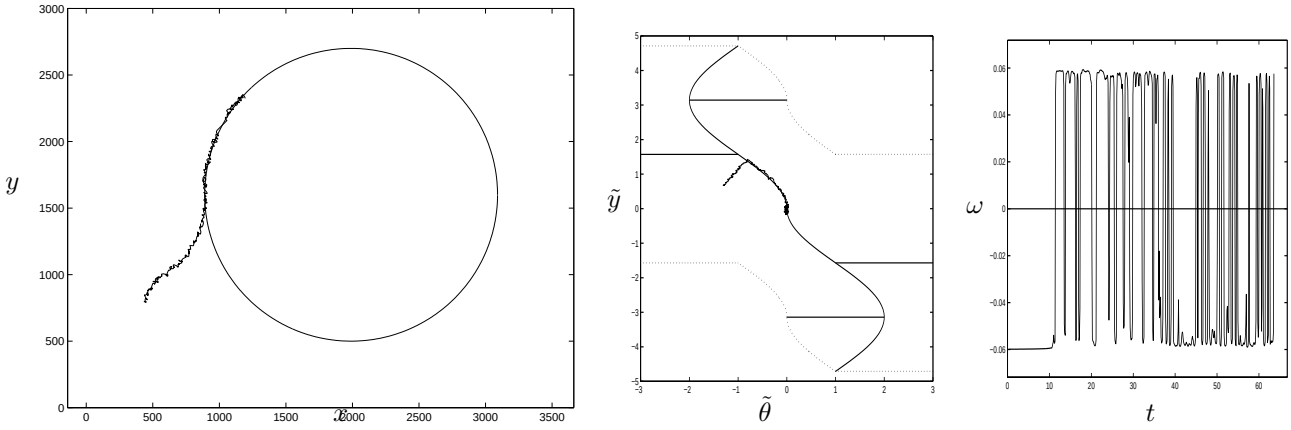

Figure 10: Data from experiment no. 1: nominal path and trajectory reconstructed by sensors (left); trajectories in the reduced state space (middle); control activity in time (right).

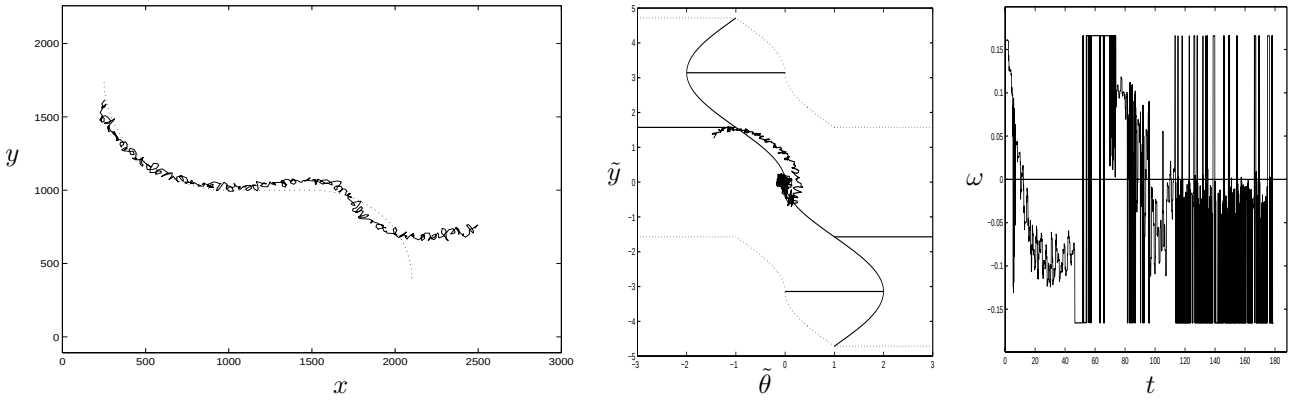

Figure 11: Data from experiment no. 2: nominal path and trajectory reconstructed by sensors (left - vehicle moves leftward); trajectories in the reduced state space (middle); control activity in time (right).

and consists of a mobile vehicle (model LabMate of Transition Research Corporation) equipped with a laser-based position sensor (a SIMAN laser scanner, with internal pre-processing unit), a PC mounted on-board, and a fixed PC communicating via a radio-modem link (4800 bps). Code concerning low-level treatment of laser measurement is implemented on the processor embedded in the sensor, while the low-level feedback control laws are run by the on-board CPU. The code resident on the fixed PC implements the high level planning and GUI. The latter consists of such functions as describing the reference path, setting parameters for the sensor and controller, and collecting and processing experimental data for analysis and visualization. As in [13], the minimum turning radius is set to 25 cm. in our experiments, and forward velocity is fixed to 5 cm/sec. Information on the vehicle position and orientation is obtained by a Kalman filter processing odometric information (encoder measurement of wheel rotations) along with angular measurements given by the ladar.

In the first experiment, reported in fig. 10, a circular reference path of radius $75cm$ is tracked, starting from an external position. The vehicle approaches the reference path by a trajectory composed of two circular arcs of opposite maximum curvature, hence keeps on the path by rapidly switching among the $turn\_right$ and $turn\_left$ modes. Results of this experiment show that model nonidealities do not influence much the overall satisfactory behaviour of the system. In the second experiment, documented in fig. 11, the reference path was composed of a circular arc of radius 60cm, a segment of length 50cm, and a circular arc of radius 75cm. The vehicle initial position is closest to the first arc. In this more challenging problem, it is possible to observe some

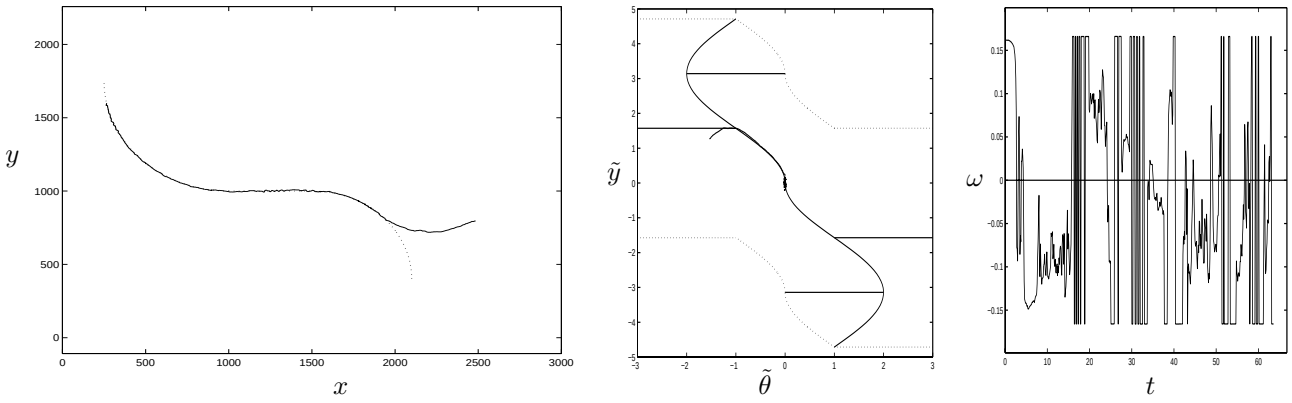

Figure 12: Data from experiment no. 3: nominal path (same as in experiment 2) and trajectory reconstructed by sensors (left); trajectories in the reduced state space (middle); control activity in time (right).

interesting effects of unmodelled phenomena. Indeed, vehicle and actuator dynamics are such that the actual angular velocity of the vehicle does not take values in the nominal set $\{0, \pm V/R\}$, rather is an interpolate thereof. Even more important is the effect of implementing the proposed control scheme, requiring very high control activity, on a platform with limited loop bandwidth, such as due in this case to computational and communication limitations. These effects are such that the system misses hooking up to the sliding surface at first transversal.

The latter problem is akin to what is known in the sliding mode literature as "chattering" ([15]), and can be reduced by standard saturation techniques (see e.g. [11]), which effectively introduce thin "boundary layers" about lines of control discontinuity in state space. Although a thorough treatment of the new system arising from modifying the proposed controller by introducing a further region in the state space for modelling the boundary layer is potentially complex, and not studied yet, it is to be expected from experience in sliding control that a degree smoothing in the switching control law would not alter the general behaviour and performance. That this is the case in the experimental setup above is indeed shown in fig. 12.

6 Acknowledgements

Support to A. Balluchi by EC grant IST-2001-33520 "CC". Support to A. Bicchi from EC (grant IST 2001-37170 "RECSYS"), and from MIUR (grants PRIN 095297_002-2002 and FIRB RBAU01RY47).

7 Conclusions

In this paper, we have used modern techniques developed for hybrid systems simulation and verification to solve and prove stability of a closed-loop control strategy a difficult problem, that is route tracking by nonholonomic vehicles with bounds on the curvature and limited sensory information. The proposed controller is reminiscent of a synthesis proposed elsewhere for an optimal control problem to track straight routes, whose generalization to generic routes turned out to be difficult to analyze otherwise. We believe that this case study, besides its intrinsic interest in applications, also has a value in showing the potential of hybrid systems analysis techniques as applied to complex control problems.

References

[1] E. Asarin, T. Dang, O. Maler, and O. Bournez, *Approximate reachability analysis of piecewise–linear dynamical systems*, in Third International Workshop, HSCC2000, Hybrid Systems: Computation and

Control, N. Lynch and B. Krogh, eds., vol. 1790 of Lecture Notes in Computer Science, Springer-Verlag, New York, U.S.A., 2000, pp. 20–31.

[2] A. Balluchi, L. Benvenuti, M. D. Di Benedetto, C. Pinello, and A. L. Sangiovanni-Vincentelli, *Automotive engine control and hybrid systems: Challenges and opportunities*, Proceedings of the IEEE, 88, "Special Issue on Hybrid Systems" (invited paper) (2000), pp. 888–912.

[3] A. Balluchi, L. Benvenuti, H. Wong-Toi, T. Villa, and A. L. Sangiovanni-Vincentelli, *Controller synthesis for hybrid systems with lower bounds on event separation*, in Proc. 38th IEEE Conference on Decision and Control, Phoenix, Arizona, USA, December 1999, pp. 3984–3989.

[4] A. Balluchi, P. Souères, and A. Bicchi, *Hybrid feedback control for path tracking by a bounded-curvature vehicle*, in Hybrid Systems: Computation and Control, M. D. Di Benedetto and A. L. Sangiovanni-Vincentelli, eds., vol. 2034 of Lecture Notes in Computer Science, Heidelberg, Germany, 2001, Springer-Verlag, pp. 133–146.

[5] L. E. Dubins, *On curves of minimal length with a constraint on average curvature and with prescribed initial and terminal positions and tangents*, American Journal of Mathematics, 79 (1957), pp. 497–516.

[6] T. A. Henzinger, *Hybrid automata with finite bisimulations*, in ICALP'95: Automata, Languages, and Programming, Z. Fülöp and F. Gécseg, eds., Springer–Verlag, 1995, pp. 324–335.

[7] J. Laumond, S. Sekhavat, and F. Lamiraux, *Robot motion planning and control*, Springer-Verlag, Berlin, Germany, 1998.

[8] J. Lygeros, C. Tomlin, and S. Sastry, *Controllers for reachability specifications for hybrid systems*, Automatica, 35 (1999).

[9] A. Olivero, J. Sifakis, and S. Yovine, *Using abstractions for the verification of linear hybrid systems*, in Proceedings of Sixth International Conference on Computer-Aided Verification (CAV-94), Springer-Verlag, 1994, pp. 81–94. Lecture Notes in Computer Science 818.

[10] C. Samson, *Control of chained systems application to path following and time–varying point–stabilization of mobile robots*, IEEE Transaction on Automatic Control, 40 (1995), pp. 64–77.

[11] J. Slotine and S. Sastry, *Tracking control of nonlinear systems using sliding surfaces with applications to robot manipulators*, International Journal of Control, 38 (1983), pp. 465–492.

[12] O. Sordalen and C. C. de Wit, *Exponential control law for a mobile robot: Extension to path following*, IEEE Transactions on Robotics and Automation, 9 (1993), pp. 837–842,.

[13] P. Souères, A. Balluchi, and A. Bicchi, *Optimal feedback control for line tracking with a bounded-curvature vehicle*, Int. Journal of Control, 74 (2001), pp. 1009–1019.

[14] D. Tilbury, O. Sordalen, L. Bushnell, and S. Sastry, *A multi-steering trailer system: conversion into chained form using dynamic feedback*, IEEE Transactions on Robotics and Automation, 11 (1995), pp. 807–18.

[15] V. Utkin, *Variable structure systems with sliding modes: a survey*, IEEE Transations on Automatic Control, 22 (1977), pp. 212–222.

[16] J. Zhang, K. Johansson, J. Lygeros, and S. Sastry, *Dynamical systems revisited: Hybrid systems with zeno executions*, in Third International Workshop, HSCC2000, Hybrid Systems: Computation and Control, N. Lynch and B. Krogh, eds., vol. 1790 of Lecture Notes in Computer Science, Springer-Verlag, New York, U.S.A., 2000, pp. 451–464.